Ocean Sci., 21, 2849–2872, 2025 https://doi.org/10.5194/os-21-2849-2025 © Author(s) 2025. This work is distributed under the Creative Commons Attribution 4.0 License.





When storms stir the Mediterranean depths: chlorophyll *a* response to Mediterranean cyclones

Giovanni Scardino^{1,2}, Alok Kushabaha^{1,3}, Mario Marcello Miglietta⁴, Davide Bonaldo⁵, and Giovanni Scicchitano^{1,2}

Correspondence: Giovanni Scardino (giovanni.scardino@uniba.it)

Received: 8 July 2025 - Discussion started: 18 July 2025

Revised: 23 September 2025 – Accepted: 12 October 2025 – Published: 11 November 2025

Abstract. Mediterranean cyclones induce significant biogeochemical perturbations in the Mediterranean Sea, with particularly notable effects on chlorophyll a (Chl a) dynamics. This study examines Chl a variability during twenty Mediterranean cyclones, comparing offshore and nearshore responses. Through an integrated investigation of reanalysis products, ARGO float observations, and Sentinel-2 multispectral satellite imagery, we quantified vertical and surface Chl a concentrations, while concurrently assessing nitrate distribution, currents, and mixed layer depth (MLD) variability. Our results revealed that both tropical-like cyclones and extratropical cyclones generated a pronounced uplift of the deep chlorophyll maximum (DCM) in cyclones exhibiting slow-moving phases. Notably, wind-driven upwelling and air-sea heat exchange critically govern DCM uplift for these cyclones. We demonstrated that these physical mechanisms collectively drive DCM uplift along the trajectories of intense, slow-moving Mediterranean cyclones, with significant implications for nutrient cycling and primary productivity across the Mediterranean basin.

1 Introduction

The dynamics of biogeochemical factors in the oceans are influenced by extreme weather events. In particular, changes in chlorophyll and phytoplankton concentrations have been widely studied to better understand upper-ocean physical properties in response to severe weather (e.g. Gallisai et

al., 2016; Karagiorgos et al., 2023). Among the intense weather systems in the Mediterranean basin, tropical-like cyclones (TLCs) and extratropical cyclones (ECs) are key drivers of alterations in the upper-ocean physical properties (Kotta, 2023; Kotta and Kitsiou, 2019a, b). Mediterranean TLCs (also known as medicanes; Miglietta et al., 2025) represent weather systems characterized by the presence of a warm core due to air-sea interaction processes and the release of latent heat, similarly to tropical cyclones, thus differing from cold core ECs (Miglietta, 2019; Miglietta and Rotunno, 2019; Panegrossi et al., 2023). Both medicanes and intense ECs are the cause of physical and biological oceanographic perturbations through intense winds and heavy rainfall (Jangir et al., 2023, 2024). Their powerful winds drive localized mixing, transporting nutrients into the upper ocean and stimulating phytoplankton blooms (Kotta, 2023; Latha et al., 2015; Lin, 2012). As for tropical cyclones, a decrease in sea surface temperature (SST) is observed after TLC passage (Avolio et al., 2024; Scardino et al., 2024), due to upwelling, vertical mixing, together with cooling due to heat fluxes towards the atmosphere (Kassis and Varlas, 2021; Menna et al., 2023; Price, 1981; Sanford et al., 1987). Vertical mixing (in particular at the base of the mixed layer), upwelling, and divergent geostrophic currents both cause shoaling of the mixed layer depth (MLD) in the water column at to the location of cyclone centre (Piontkovski and Al-Hashmi, 2014). This, in turn, induces the upward transport of nutrients, favouring higher biological productivity (Kotta and Kitsiou, 2019a, b; Piontkovski and Al-Hashmi, 2014). When these

¹Department of Earth and Geoenvironmental Sciences, University of Bari Aldo Moro, 70125 Bari, Italy

²Interdepartmental Research Centre for Coastal Dynamics, University of Bari Aldo Moro, 70125 Bari, Italy

³IUSS – School for Advanced Studies, Pavia, Italy

⁴Institute of Atmospheric Sciences and Climate (CNR-ISAC), National Research Council of Italy, Padua, Italy

⁵Institute of Marine Sciences (CNR-ISMAR), National Research Council of Italy, Venice, Italy

nutrients reach the sunlit euphotic zone – combined with adequate light for photosynthesis – chlorophyll a (Chl a) concentrations increase significantly (Latha et al., 2015). Generally, strong, slow-moving cyclones can induce significant sea surface cooling and phytoplankton blooms (Lin, 2012; Mei et al., 2015; Wang, 2020; Zhao et al., 2008). These intense weather systems can also produce prolonged precipitation lasting several days (Owen et al., 2021; Tartaglione et al., 2006), altering the Chl a concentrations in the Mediterranean Sea (Katara et al., 2008; Kotta et al., 2017).

The Mediterranean Sea is defined as an oligotrophic basin, with generally low nutrient availability and consequently low phytoplankton biomass (D'Ortenzio and Ribera d'Alcalà, 2009). Chl *a*, a proxy for phytoplankton biomass, exhibits strong spatial and temporal variability due to the interplay of oceanographic processes (Mélin et al., 2017). In the Mediterranean open sea, low Chl *a* concentrations (0.05–0.3 mg m⁻³) are typically observed in the first meters of the water column, due to nutrient limitation (Li et al., 2024b; Marty and Chiavérini, 2010, 2002; Teruzzi et al., 2021). However, the coastal zones and river-influenced regions (e.g., near the Nile Delta, Rhône, or Po River outflows) exhibit higher Chl *a* concentrations (0.5–5 mg m⁻³) at the surface (Fig. 1), due to terrestrial nutrient inputs (Ludwig et al., 2009).

While the warming of the Mediterranean Sea surface is a well-established pattern (Belkin, 2009; Rixen et al., 2005; Skliris et al., 2012), the dynamics of phytoplankton, especially in response to meteorological forcings, are less clear. Chl *a* changes due to the occurrence of Mediterranean cyclones are not well understood yet. Other severe weather events may affect the dynamics of nutrients, Chl *a* and deep chlorophyll maximum (DCM) differently, depending on the specific weather system (Kotta, 2023; Kotta and Kitsiou, 2019b; Walker et al., 2005).

A defining characteristic of phytoplankton dynamics in the Mediterranean Sea is the presence of a DCM, which typically forms near the base of the euphotic zone, aligned with the upper nutricline in both permanently and seasonally stratified waters (Cullen, 2015). Below the nutricline depth (more than 120 m), the concentrations of nitrate and phosphate increase (Lazzari et al., 2016; Mignot et al., 2019). Satellite-derived data revealed an increase in the Chl a concentration after the passage of medicanes, as observed after medicane Zeo (12-15 December 2005; Kotta and Kitsiou, 2019b) and medicane Ianos (15-20 September 2020; Kotta, 2023). Menna et al. (2023) observed an uplift of DCM during the occurrence of medicane Apollo (25 October-1 November 2021), concomitant with a shoaling of the nutricline and MLD. They described a sort of dome shape near the cyclone eye, where all vertical profiles of biogeochemical parameters were shoaled. Generally, the shoaling of biogeochemical parameters during the occurrence of strong Mediterranean cyclones seems to be associated with subsurface water mixing and wind-driven upwelling (Jangir et al., 2024; Mourre et al., 2023; Zhang et al., 2021).

Jangir et al. (2024) highlighted increased Chl a and phytoplankton concentrations at the warm-core eddy locations for medicane Apollo. However, Kassis and Varlas (2021) reported a deepening in the MLD during the occurrence of medicane Zorbas (26–29 September 2018), caused by the inflow of Atlantic currents. Nonetheless, this event experienced an increase in Chl a and phytoplankton concentration by approximately 0.01 mg m $^{-3}$ and 0.02 mmol m $^{-3}$, respectively (Jangir et al., 2024).

In this study, we analysed the Chl a variations throughout the water column and at the sea surface during intense TLCs and ECs. We selected twenty cyclones based on their intensity, estimated using mean sea-level pressure (MSLP) and heat flux values from the ERA5 and Copernicus reanalysis dataset. Quasi-stationarity and slow-movement phases were assessed by tracking the MSLP minima for each event. Using remote sensing data and reanalysis products, we evaluated Chl a concentrations in areas affected by slow-moving cyclone phases and along the impacted coastal regions. Subsequently, we correlated these variations with key biogeochemical variables, including nitrate distribution, currents, MLD, and downward heat flux. Although previous studies have analysed a similar topic in other basins, this is the first time the issue has been analysed in a systematic way in a peculiar basin as the Mediterranean.

The paper is organized as follows. Section 2 describes the materials and methods used to analyse Chl *a* changes during Mediterranean cyclones. In particular, we assess the relationship between the translation speed and intensity of cyclones and their impact on Chl *a* variations. Section 3 presents the results of our analysis, highlighting the uplift of the DCM and its association with changes in biogeochemical variables, such as nitrate concentrations, current distributions, and MLD deepening/shoaling. Section 4 discusses the correlation between DCM uplift and physical variables during different cyclone events, with a particular focus on DCM dynamics in the cyclone's centre and periphery. The main findings are reported in Sect. 5.

2 Material and methods: analysis of chlorophyll *a* changes during Mediterranean cyclones

In this study, we analysed multiple datasets to reconstruct Chl *a* dynamics in response to Mediterranean cyclone forcing. The following steps were undertaken:

- assessment of slow-moving phases and heat energy seaward of the cyclones;
- analysis of Chl a dynamics in offshore and nearshore regions;
- joint analysis of Chl a dynamics with biogeochemical variables.

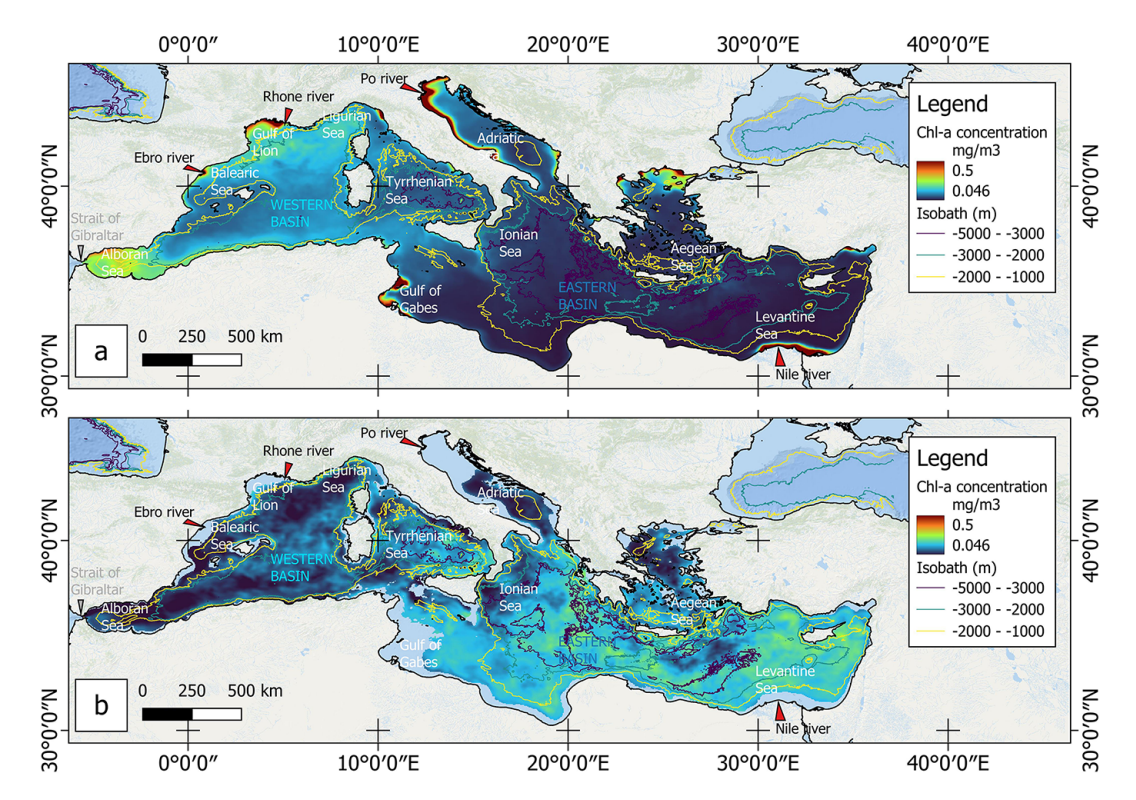


Figure 1. Chlorophyll concentration in the Mediterranean basin extracted from Copernicus yearly dataset (in the map data refer to 2022); (a) surface Chl *a* concentration; (b) Chl *a* concentration extracted below the nutricline water depth (i.e. Chl *a* concentration at 120 m). The areas where sea depth is below 120 m are in cyan. Figure contains the background maps provided by Esri World Ocean Basemap (sourced from Esri's ArcGIS Online services.).

To capture the full temporal evolution of biogeochemical variables during the cyclone passage, we analysed Sentinel-2 and ARGO data alongside ERA5 (hourly data) and CMEMS (daily data) reanalysis products. This approach provided a comprehensive overview of the event's progression, particularly revealing time-series variations in MLD and DCM dynamics.

2.1 Identifying the areas influenced by Mediterranean cyclones and associated Chl *a* changes

To identify the cyclone-impacted regions and the movement of the cyclones, we extracted hourly minimum MSLP values from ERA5 reanalysis data $(0.25^{\circ} \times 0.25^{\circ}$ resolution) for the cyclones listed in Table 1. The cyclone-impacted areas were selected following the literatures, focusing on those areas greatly affected by wind stress (Table 1). The selected areas for each cyclone are reported in the Supplement S1. Slow-moving phases were evaluated by tracking the displacement of hourly MSLP minima. According to Piontkovski and Al-Hashmi (2014), slow cyclones, characterized by a translation speed lower than $10 \, \mathrm{m \, s^{-1}}$, are able to induce Chl a changes. Events exhibiting displacements shorter than 36 km over 4 h were considered as slow-moving cyclone phases (these phases are underlined by the red shaded areas reported

in Fig. 2 for the case of medicane Zorbas). While, quasistationary phases have been considered for the displacements shorter than 10 km over 4 h.

Then, we analysed the MSLP minima alongside daily surface downward heat flux in sea water (hfds), extracted from Copernicus reanalysis (Clementi et al., 2019; Escudier et al., 2020) at $0.04^{\circ} \times 0.04^{\circ}$ resolution to map the regions where air–sea interaction is more intense and may influence the cyclone dynamics.

Wind data from ERA5 were extracted in the following two components: the eastward wind component (U wind) and the northward wind component (V wind). These components were combined to obtain the wind speed during storm events as follows (Eq. 1):

Wind speed =
$$\sqrt{U^2 + V^2}$$
. (1)

To determine the cyclone-impacted area, we first identified the location of the maximum wind speed at 10 m height within a 200 km radius of the cyclone centre. The radius of maximum wind was then defined as the distance from the centre to this location. The cyclone-impacted area was subsequently assessed as a circular area with the radius of maximum wind (see Supplement S1).

The cyclones were analysed to assess the combined influence of their persistence and their associated intensity in a

Table 1. Mediterranean cyclones considered in this study for the analysis of Chl a dynamics; classification is based on the intensity variables reported in literature.

Cyclone	Dates of occurrence	Classification	Features	Reference	Impacted areas	
		Mediterranean hurricane	Deep warm core; flash floods Fita et al. (2007), Gutiérrez-Fernández al. (2024), Kotta and Kitsiou (2019b), Miglietta and Rotunr (2019)		V V V	
Janet – 2007	13–19 October 2007	Extratropical cyclone		Flaounas et al. (2022)	Libya	
Rolf – 2011	6–9 November 2011	Mediterranean hurricane	Eye-like structure; 6 November 2011: asymmetric deep cold core; 7–8 November 2011: deep warm core	Cavicchia et al. (2014), Ricchi et al. (2017), de la Vara et al. (2021)	Gulf of Lyon (France), Corsica, northwestern Italy	
Akle – 2011	2–3 January 2011	Mediterranean Tropical Storm	Shallow warm core	Flaounas et al. (2022, 2023)	Southeastern Sicily, Greece	
Qendresa – 2014	7–9 November 2014	Mediterranean hurricane	Rapid intensification; > 100 mm rainfall in Malta	Carrió (2023), Pytharoulis (2018)	Malta, Sicily, eastern Tunisia	
Xandra – 2014	1–4 December 2014	Mediterranean Tropical Storm	Weak warm core	Di Muzio et al. (2019)	Western Mediterranean; Tyrrhenian Sea	
Erik – 2015	21–22 May 2015	Mediterranean Tropical Depression	Shallow warm core	Flaounas et al. (2023)	Ionian Sea	
Trixie – 2016	28 October–1 November 2016	Mediterranean hurricane	Deep warm core	Dafis et al. (2020), Di Francesca et al. (2025), Saraceni et al. (2023)	Ionian Sea, western Greece	
Caulonia – 2016	16–17 March 2016	Mediterranean Tropical Depression	Shallow warm core	Flaounas et al. (2023)		
Numa – 2017	15–19 November 2017	Mediterranean hurricane	Deep warm core	Marra et al. (2019), Tiesi et al. (2021)	Adriatic Sea, Greece, Albania	
Zorbas – 2018	27–29 September 2018	Mediterranean hurricane	27 September 2018: deep cold core 28 September 2018: deep symmetric warm core	de la Vara et al. (2021)	Southeastern Sicily; Peloponnese area	
Vaia – 2018	27–29 October 2018	Extratropical cyclone	Explosive Davolio et al. (2020), cyclogenesis; Federico et al. (2021), Giovannini et al. (2021)		Ligurian coasts; North Adriatic	
Trudy – 2019	11–13 November 2019	Mediterranean Tropical Storm	Deep warm core	Listowski et al. (2022)	Balearic Islands	

Table 1. Continued.

Cyclone	Dates of occurrence	Classification	Features	Reference	Impacted areas
Ianos – 2020	15–20 September 2020	Mediterranean hurricane	Deep warm core	Comellas Prat et al. (2021), D'Adderio et al. (2022), Jangir et al. (2024), Lagouvardos et al. (2022)	Ionian Islands, western Greece
Apollo – 2021	25 October–1 November 2021	Mediterranean hurricane	Shallow warm core	Menna et al. (2023), Panegrossi et al. (2023)	Sicily (Italy), Malta
Blas – 2021	6–18 November 2021	Mediterranean hurricane	Shallow warm core	Mourre et al. (2023)	Balearic Islands; Spain, Algeria
Ciprian – 2022	16–20 October 2022	Extratropical cyclone		Scardino et al. (2024)	Cyprus Island
Helios – 2023	8–11 February 2023	Mediterranean hurricane	8–9 February 2023: Deep cold core; 10 February 2023: warm core	D'Adderio et al. (2023)	Southeastern Sicily
Juliette – 2023	28 February–2 March 2023	Mediterranean hurricane		D'Adderio et al. (2023)	Balearic Islands, Sardinia (Italy)
Daniel – 2023	6–12 September 2023	Mediterranean hurricane	6 September 2023: Cold core; 8 September 2023: deep warm core	Argüeso et al. (2024), Flaounas et al. (2024)	Greece, Turkey, and Libya

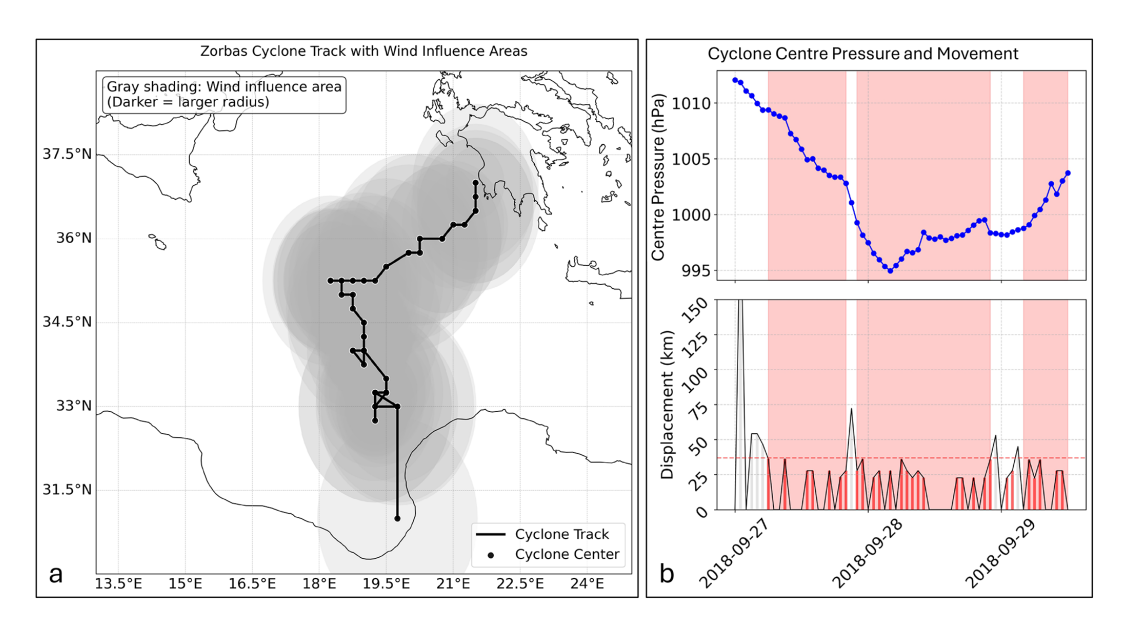


Figure 2. Assessment of the stationarity phase of a cyclone from MSLP data (case of medicane Zorbas); (a) extraction of minimum MSLP point with value of centre (minimum) pressure and the maximum wind speed at 10 m height within a 200 km radius from the cyclone centre (gray shading areas); (b) centre pressure along the cyclone track and displacements assessed across each minimum MSLP point, red bars indicate the displacement when it was shorter than 36 km in 4 h, while shaded red areas indicate the long lasting slow-moving phases.

given area. To determine the total energy changes during cyclone events, a double integral was applied to the hfds within cyclone-affected areas:

$$Q_{\text{total}}(t) = \int \int_{A} \text{hfds}(x, y, t) dx dy$$
 (2)

$$E_{\text{total}} = \int_{t_1}^{t_2} Q_{\text{total}}(t) dt.$$
 (3)

 $Q_{\text{total}}(t)$ is equal to the total heat flux over area A at time t (units: W). Equation (2) provides the instantaneous power (energy per second) entering or leaving the Mediterranean Sea over a given region (specifically the areas affected by Chl a changes). E_{total} represents the total energy change over time (units: J). Equation (3) provides the net heat gained or lost by the ocean region during cyclone lifetime, i.e., between t_1 (here 1 d before cyclogenesis) and t_2 (here 1 d after cyclolysis).

2.2 Variations of Chl a in offshore and nearshore areas

The analysis of Chl *a* focused on the main variations observed offshore and in nearshore areas that were greatly impacted by cyclones. For this study, the nearshore was defined as the buffer zone from the coastline to the global average depth of closure of 13 m (Athanasiou et al., 2019). The coastline data were obtained from the European Environment Agency, and the depth data were extracted from the GEBCO bathymetric grid (GEBCO, 2020).

Offshore, the focus was on the variations in the DCM, using two kinds of datasets:

- Biogeochemistry variables from Copernicus reanalysis products (Cossarini et al., 2021) used to assess Chl a changes via cross-section analysis and vertical profiles across different cyclone phases (from cyclogenesis to cyclolysis).
- ARGO float observational data (https://dataselection. euro-argo.eu/, last access: 1 July 2025) used to provide vertical Chl a profiles within a variable time range (from 1 d before cyclogenesis to 1 d after cyclolysis) down to a water depth of 500 m.

An uncertainty assessment of reanalysis products was performed, calculating the root mean square error (RMSE) in comparison with the observational data of the ARGO float (Fig. 3 and Supplement S2).

The analysis of Chl *a* vertical profiles was performed by measuring the difference in water depth of the DCM, in order to highlight uplift and downlift movements of the DCM.

Subsequently, the DCM uplift/downlift was assessed across the entire cyclone-affected area through a spatial analysis of DCM differences between pre-cyclone conditions and after the cyclone's lifetime.

Horizontal patterns of Chl *a* concentrations in the nearshore were derived from Sentinel-2 MSI data using the C2RCC (Case-2 Regional CoastColour) processor in ESA's SNAP software, which applies a neural-network-based atmospheric correction and inherent optical property (IOP) inversion to estimate water constituents in optically complex waters. Prior to chlorophyll retrieval, Sentinel-2 Level-1C top-of-atmosphere (TOA) radiance data were preprocessed with C2RCC, which incorporates a bio-optical model to derive water-leaving reflectances and subsequently estimate Chl *a* concentrations through IOP inversion. Sentinel 2 images were selected prior to the cyclone onsets and after the cyclone impact, in order to highlight the changes in Chl *a* caused by rainfall and the dynamics of surface currents.

2.3 Joint analysis of Chl a variations and biogeochemical variables

To better understand the mechanisms influencing Chl a and DCM dynamics, biogeochemical (such as nitrate distribution) and physical variables (currents and MLD) were overlaid with the Chl a concentration and DCM depth to identify upwelling/downwelling effects. Currents were extracted from Copernicus reanalysis (MED-SEA_MULTIYEAR_PHY_006_004; Clementi et al., 2019; Escudier et al., 2020), considering eastward (u_0) and northward (v_0) sea water velocities up to 500 m of the water column. These components were combined to obtain the current speed in the cross-section:

Current speed =
$$\sqrt{u_0^2 + v_0^2}$$
. (4)

This approach highlights how DCM dynamics respond to the cyclone passage in different locations. Additionally, MLD maps were plotted by comparing surface MLD values 1 d before and 1 d after each cyclone event, in order to correlate changes in DCM with shoaling/deepening of MLD. A spatial difference between the two MLD surfaces was performed for the entire Mediterranean basin following the relationship (Eq. 5):

$$\begin{aligned} \text{sign}\left(\text{MLD}_{\text{dif}}\right) &= \\ \left\{ \begin{array}{ll} \text{deepening} & \text{if } \text{MLD}_{\text{dif}} = \text{MLD}_{t_2} - \text{MLD}_{t_1} \geq 0 \\ \text{shoaling} & \text{if } \text{MLD}_{\text{dif}} = \text{MLD}_{t_2} - \text{MLD}_{t_1} < 0 \end{array} \right. \end{aligned} \tag{5}$$

where $sign(MLD_{dif})$ reports the sign of the difference of MLD; MLD_{t_2} indicates the MLD values at the end of cyclone lifetime; MLD_{t_1} indicates the MLD values 1 d before the cyclone onset.

In this way, negative values are representative of MLD shoaling, while positive values are representative of MLD deepening.

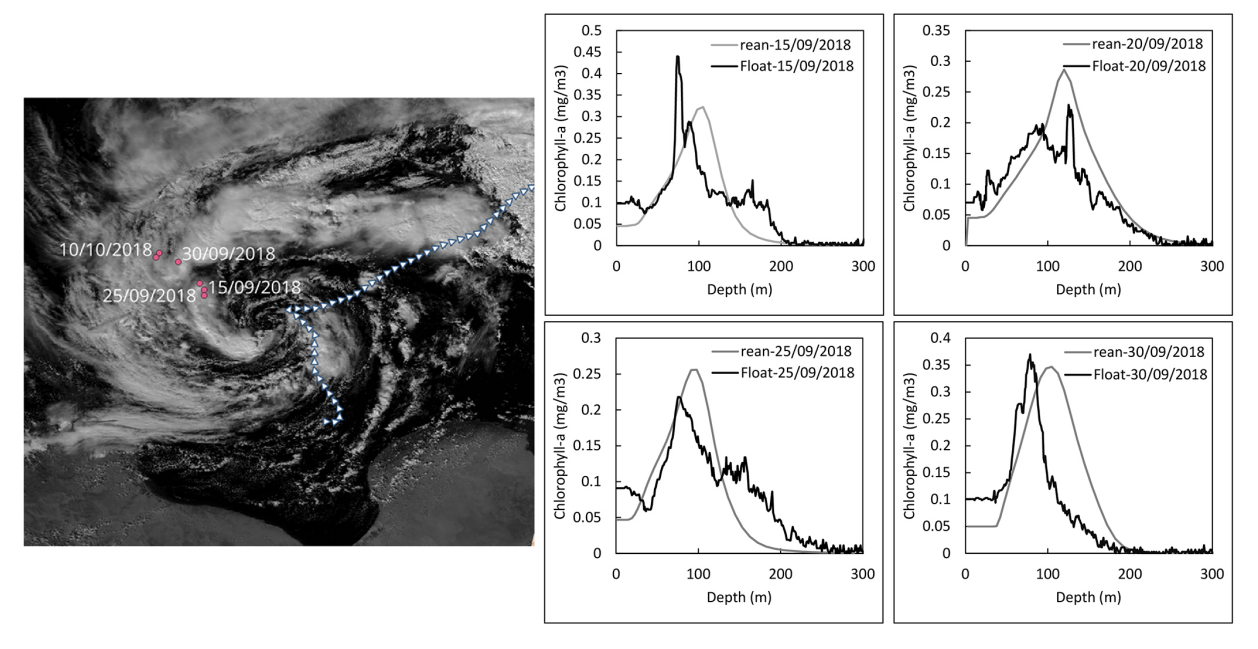


Figure 3. Comparison between reanalysis products (rean-date in the panels) and ARGO float data (float-date in the panels) for the medicane Zorbas occurred in the Ionian Sea (satellite image from MODIS/Aqua Surface Reflectance available at https://search.earthdata.nasa.gov, last access: 1 July 2025); the Chl *a* profiles from reanalysis were extracted in the same location as the float measurements.

3 Results

3.1 Translation speed of the Mediterranean cyclones

The reanalysis products enabled assessment of key intensity variables influencing Chl *a* dynamics. Specifically, we extracted and tabulated maximum wind speed, MSLP minima, and translation speed in Table A1.

The analysis of the MSLP minima revealed several slow-movement phases in the TLCs and ECs lifetime (Supplement S1). Cyclones characterized by slow-moving phases and by a significant intensity revealed the greatest changes in the Chl *a* concentrations. In particular, a DCM uplift appeared for the most intense, slow-moving phases of the cyclones.

For example, medicane Zorbas exhibited different phases of movement:

- a first slow-movement phase from 27 September, 10:00 UTC to 27 September 2018, 17:00 UTC,
- a second, slow-moving phase from 27 September, 18:00 UTC to 28 September 2018, 18:00 UTC,
- a third slow-moving phase from 29 September, 00:00 UTC to 29 September 2018, 07:00 UTC.

During the second and final quasi-stationary phase, medicane Zorbas reached its maximum intensity, characterized by low MSLP values (below 997.5 hPa). A similar behaviour was observed for medicanes Ianos and Apollo (Fig. 4b and c):

- medicane Ianos displayed very slow movement in its most intense phase, from 16 September, 17:00 UTC to 19 September 2020, 05:00 UTC;
- medicane Apollo showed an initial slow-movement phase from 28 October, 14:00 UTC to 28 October 2021, 21:00 UTC, followed by another slow-moving phase lasting from 29 to 30 October 2021, 05:00 UTC.

Among the other cyclones considered in this study, some extratropical cyclones – Janet (November 2007), and Ciprian (October 2022) – exhibited slow movement in their most intense phases (Supplement S1). Other extratropical cyclones, such as Vaia, did not experience a slow-moving phase and therefore no significant DCM uplift was observed.

3.2 Heat fluxes and biogeochemical variables

The integrated analysis of ERA5 and Copernicus reanalysis data revealed a sharp intensification (in absolute values) in downward heat fluxes (ranging from -210 to -700 W m⁻²) during the cyclogenesis and most intense phase of TLCs. The most extreme intensifications were observed for medicane Zorbas (extreme of -606 W m⁻²) and Qendresa (extreme of -655 W m⁻²), coinciding with their peak intensities (Table 2). However, medicane Qendresa showed a short quasi-stationarity phase differently from medicane Zorbas. Weaker Mediterranean storms (e.g., Akle-2011, Erik-2015) exhibited weaker heat fluxes anomalies.

A general shoaling of biogeochemical variables was observed concurrently with the intensification of the heat fluxes

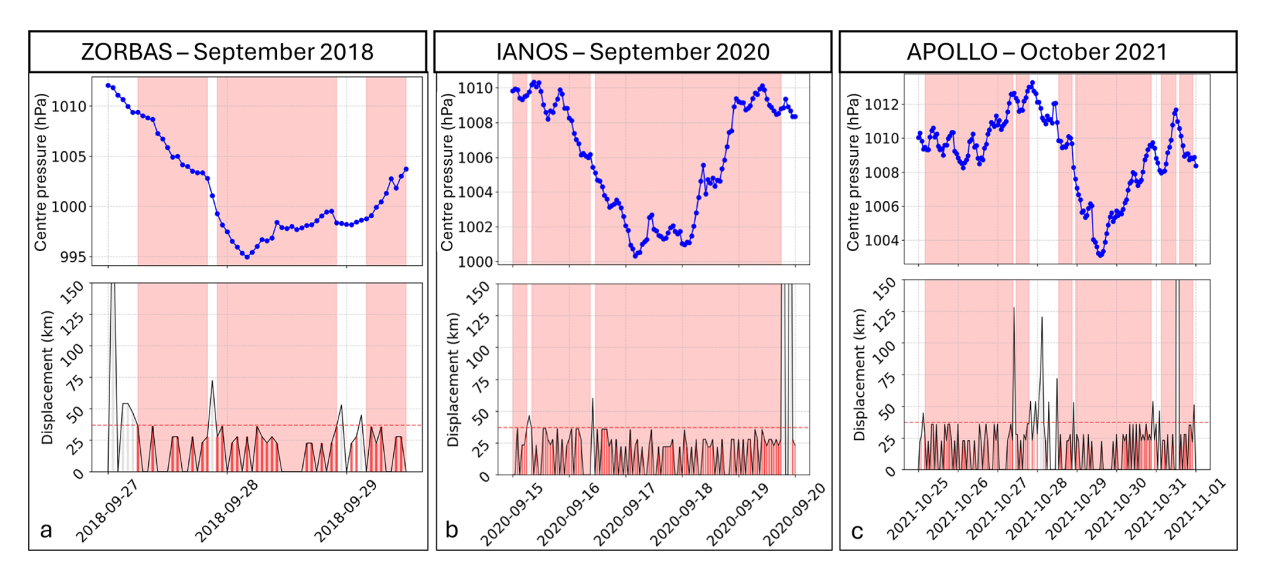


Figure 4. MSLP minima displacement tracked along medicane trajectories, with graphs showing time series of central (minimum) pressure and relative displacement. Slow-moving phases (red rectangles) are illustrated for: (a) Zorbas, (b) Ianos, and (c) Apollo.

Table 2. Values of heat fluxes and total heat lost within the region affected by Chl *a* changes for each cyclone.

Cyclone	Day	Minimum	Total
	,	value	heat
		of heat	lost
		flux	within
		during	the
		the	region
		cyclone	affected
		occurrence	by Chl a
		$({\rm W}{\rm m}^{-2})$	changes
			$(10^{18} \mathrm{J})$
Zeo – 2005	11 December 2005	-386	-41.6
Janet – 2007	13 October 2007	-255	-37.7
Akle – 2011	1 January 2011	-139	-5.39
Rolf – 2011	5 November 2011	-317	-11.6
Qendresa - 2014	7 November 2014	-655	-26.2
Xandra – 2014	30 November 2014	-260	-19.2
Erik – 2015	21 May 2015	102	10.9
Caulonia – 2016	16 March 2016	36	1.45
Trixie – 2016	27 October 2016	-269	-45
Numa – 2017	13 November 2017	-300	-64.3
Zorbas – 2018	26 September 2018	-606	-46.3
Vaia – 2018	29 October 2018	-334	-8.02
Trudy – 2019	11 November 2019	-546	-13.1
Ianos – 2020	14 September 2020	-268	-18.6
Apollo – 2021	27 October 2021	-210	-45.8
Blas – 2021	5 November 2021	-275	-67.9
Ciprian – 2022	12 October 2022	-181	-18.5
Helios – 2023	8 February 2023	-498	-13.1
Juliette – 2023	27 October 2023	-202	-8.22

(Supplement S4). The values of total heat lost ($E_{\rm total}$) within the region affected by the cyclone impact were obtained through the double integral of the surface downward heat flux (Eqs. 1 and 2). For the most intense cyclones, intense heat fluxes were observed, like in medicane Zorbas (-4.63×10^{19} J), medicane Numa (-6.43×10^{19} J), and medicane Blas (-6.79×10^{19} J). Conversely, weak cyclones were characterised by smaller heat loss, as happened for cyclones Akle (-5.39×10^{18} J), Erik (1.09×10^{19} J) and Caulonia (1.45×10^{18} J) (Supplement S4). Pearson's correlation coefficient r between total energy (net heat loss) and DCM uplift resulted equal to -0.64, indicating an inverse relationship, thus indicating that a greater heat loss is associated with a greater DCM uplift.

The primary changes in these biogeochemical variables were reflected in both the uplift of the DCM and patterns of alternating upwelling/downwelling currents (Fig. 5). Cross-sectional analysis further revealed that the DCM uplift was more pronounced within the cyclone centre (Fig. 5c and d). On the outskirts of the cyclone, current vectors indicate downwelling components, which determined localized downlift in deep nutrients, like nitrate.

3.3 Uplift of the deep chlorophyll maximum in Mediterranean offshore regions

Vertical profiling of Chl a from reanalysis and ARGO float data demonstrated a significant uplift of the DCM along the track of the most intense Mediterranean cyclones, particularly for those events characterized by slow-moving phases. The correlation between the number of hours of slow-moving phases and DCM uplift revealed a Pearson's r equal to 0.80, with a highly significant relationship between longer slow-moving phases and greater DCM uplift. Cyclones persisting

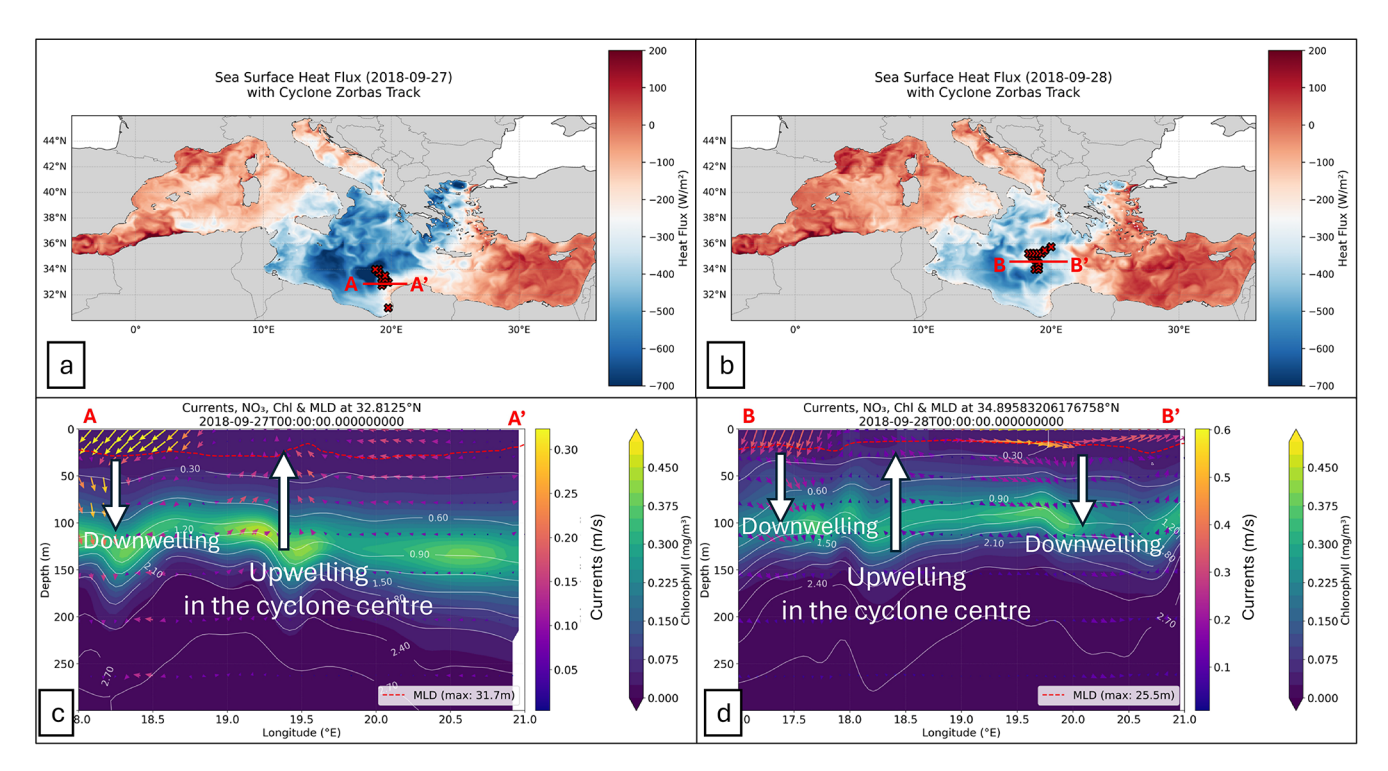


Figure 5. Heat fluxes and cross-section of biogeochemical variables during medicane Zorbas (27–29 September 2018); (**a, b**) heat fluxes maps assessed on 27 and 28 September 2018, with cross-sections marked in red (x in red indicates the minimum MSLP value recorded on each date); (**c–d**) cross-sections showing: Chl *a* concentration (viridis colormap), Nitrate concentration in mmol m⁻³ (white contour lines), Current vectors (plasma-colored arrows), Mixed layer depth (MLD, red dashed line).

in a slow-moving state cause ~ 40 –60 m DCM uplift, likely due to prolonged wind-driven mixing and upwelling. Conversely, short-duration events (less than 20 h) show minimal DCM uplift (0–10 m).

In particular, intense tropical-like cyclones, with slow-moving or quasi-stationary phases (e.g. Numa, Zorbas, Apollo, Blas, Helios), were characterized by a greater DCM uplift in their most intense phases (Fig. 6). In fact, a limited vertical (deep) wind shear is characteristic of the environment where medicanes form and develop their warm core; such conditions favour their slow movement (Cavicchia et al., 2014). Conversely, other events, comparable in intensity but less stationary, experienced lower DCM uplift (e.g. Qendresa, Vaia, Daniel). Other events, generally of weaker intensity, were characterized by an opposite behaviour, with a DCM downlift near the cyclone centre (Akle, Erik, Caulonia, Juliette).

Considering the lower resolution of the reanalysis products with respect to floats, RMSE assessments were performed to better define the significance of the DCM uplift/downlift (Supplement S2). The RMSE values were below the reanalysis vertical profile resolution (3 m). Nevertheless, for medicanes Ianos and Blas, the RMSE showed larger discrepancies in DCM depth, which were greater than 1 m.

The DCM uplift was accompanied by evidence of shoaling on biogeochemical variables. As an example, during medicane Zorbas, the DCM uplifted by 15 m (duration of 24 h) in cyclogenesis regions and 30 m in the most intense phase (duration of 68 h) (Fig. 7a and b), coinciding with intensified upwelling in the cyclone centre. Cross-sectional analysis revealed that the uplift was accompanied by:

- Enhanced nitrate concentrations (up to 0.8 mmol m⁻³) near the euphotic zone.
- MLD shoaling in the cyclogenesis and most intense phase, with reductions greater than 5 m in regions of persistent cyclone influence.
- MLD deepening along the peripheral borders of the cyclone.
- Strong vertical currents, with upwelling velocities exceeding 0.05 m s⁻¹ in the cyclone centre.

Spatial analysis of DCM changes revealed widespread uplift patterns following cyclone trajectories (Supplement S5). Medicane Zorbas exhibited particularly intense localized DCM uplift, reaching 40 m in certain areas (Fig. 8a); conversely, DCM downwelling was observed along the southeastern Sicily and Peloponnese coastal regions, where concurrent MLD deepening occurred (Fig. 8b). These MLD patterns were likely driven by a circulation associated with downwelling in the outskirts of the cyclone during its most

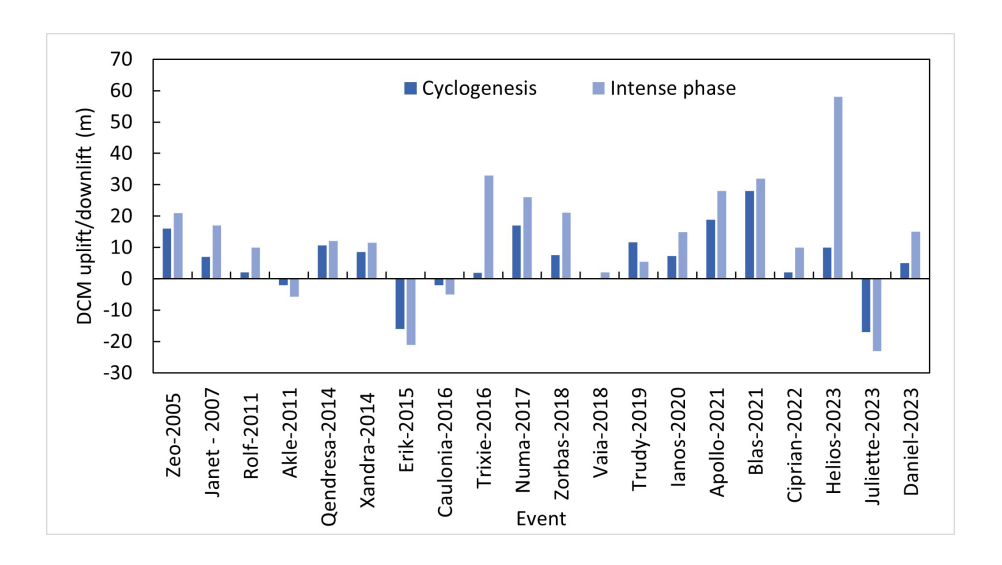


Figure 6. DCM uplift measured at the cyclone centres from the Copernicus reanalysis dataset, considering as temporal range the difference between 1 d prior to the cyclogenesis and 1 d after the cyclolysis (maximum total duration of 120 h); different bars indicate different locations (blue for the cyclogenesis and light blue for the most intense phase locations).

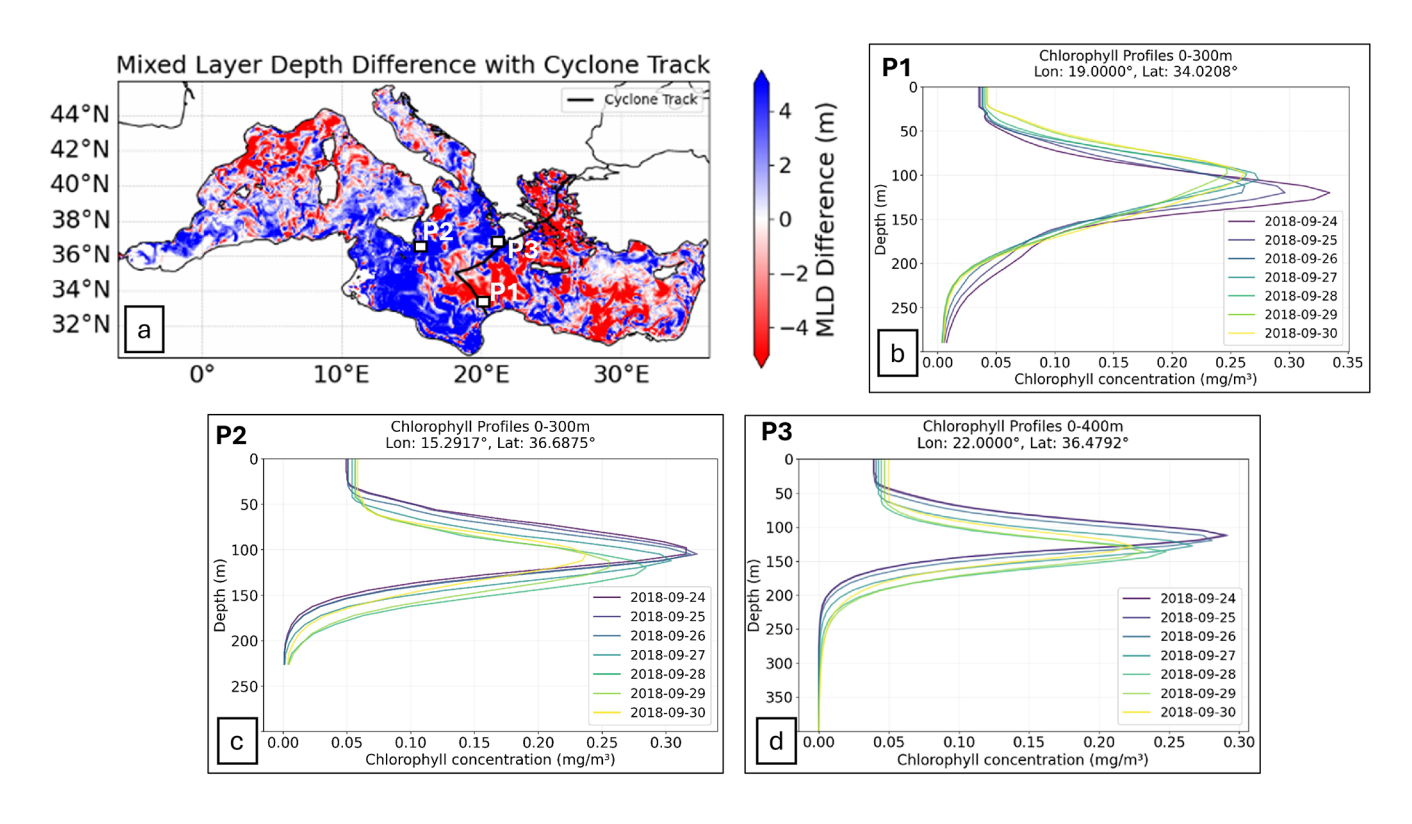


Figure 7. Spatial analysis of MLD changes and vertical Chl a concentrations derived from reanalysis products (cell resolution of $0.04^{\circ} \times 0.04^{\circ}$) during the occurrence of medicane Zorbas; (a) changes in MLD assessed from 26 to 29 September 2018, red surfaces indicate the MLD shoaling, while blue surfaces indicate the MLD deepening; (b) changes in vertical profiles of Chl a assessed in the cyclogenesis area (P1); (c) changes in vertical profile of Chl a assessed in the proximity southeastern Sicily (P2); (d) vertical profile of Chl a assessed in the proximity of Peloponnese coasts.

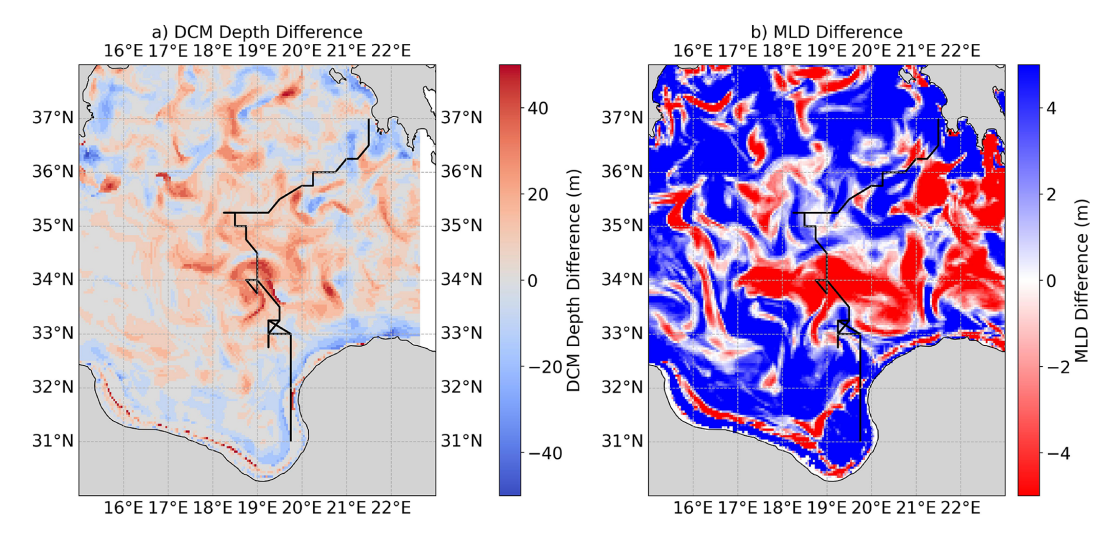


Figure 8. Spatial analysis of DCM changes during the occurrence of medicane Zorbas correlated to the MLD deepening/shoaling; (a) DCM depth difference assessed for the areas influenced by medicane Zorbas (difference between DCM at 29 September and DCM at 26 September 2018); (b) MLD difference assessed in the same period (black line indicates the cyclone track).

intense phase. Notably, Kassis and Varlas (2021) reported MLD deepening during Zorbas, contrasting with our coreregion shoaling. This discrepancy likely reflects spatial and methodological differences: their study captured basin-scale adjustments (e.g., Atlantic inflow), whereas our analysis focused on the cyclone centre, where wind-driven upwelling and heat loss dominated (Figs. 7 and 8). Kassis and Varlas (2021) noted that Atlantic water intrusion could have disrupted local upwelling, leading to net MLD deepening in offshore areas of southeastern Sicily and the Pelopponese. Chl a signal resulted to be characterized by a sustained bloom, as also highlighted in other studies (Kotta, 2023; Kotta et al., 2017; Kotta and Kitsiou, 2019b). On the other hand, the ARGO data revealed that DCM uplift persisted also after the cyclolysis in the centre of the cyclone.

3.4 Nearshore Chl *a* variability driven by runoff and surface currents

The development of intense TLCs and ECs was associated with an increase in Chl *a* concentrations along the affected coasts, due to two different kinds of features: a redistribution of suspended organic matter caused by ocean currents and an increase in sediment-laden plumes.

In particular, cyclones characterized by the absence of heavy rainfall along the coastal areas showed an increase in Chl a concentration in the nearby sea surface layer. This is the case of medicane Zorbas whose circulation impacted southeastern Sicily far from its centre. The increase in Chl a concentration appeared to be related to the redistribution of suspended organic matter from the coast toward the sea. These dynamics seem to be related to the contributions of ocean surface currents during the cyclone impact. Sentinel-2 imagery highlighted that medicane Zorbas generated a

gyre off southeastern Sicily, transporting high-Chl a waters (> 1.5 mg m⁻³) offshore (Fig. 9a and b). Conversely, areas greatly impacted by cyclone-driven rainfall highlighted plume formation several kilometers long, as observed during medicane Daniel impacting Libya (11 September 2023). This event caused extreme surface runoff with a plume formation that determined an increase of Chl a by 2–4 mg m⁻³ along Libyan coasts and over the open sea some tens of km far away (Fig. 9c and d).

4 Discussion

The analysis performed on the MSLP minima of Mediterranean cyclones revealed that slow-moving cyclones characterized by high intensity (low MSLP values and a significant amount of net heat loss) could lead to a significant variation in the biogeochemical variables. According to Piontkovski and Al-Hashmi (2014), slow-moving cyclones can drive an increase in Chl a concentration, considering a threshold for the translation speed of $36 \,\mathrm{km}\,\mathrm{h}^{-1}$. In our case, we considered a similar threshold of 36 km/h assessed through ERA5 MSLP hourly data. Pearson correlation revealed a positive correlation between the duration of slowmoving phases and DCM uplift (Fig. 10a). Prolonged durations (e.g., Ianos-2020; 79 h) drive up to 20-60 m of DCM uplift, while short-lived stationary phases (e.g., Rolf-2011; 9h) show minimal effect. Additionally, a prolonged persistence of strong cyclones can determine heavy rainfall in a given location, favouring vertical mixing in seawater and increasing phytoplankton blooms (Owen et al., 2021; Vargas-Yáñez et al., 2022), and also influencing the productivity during the spring season (Li et al., 2024a).

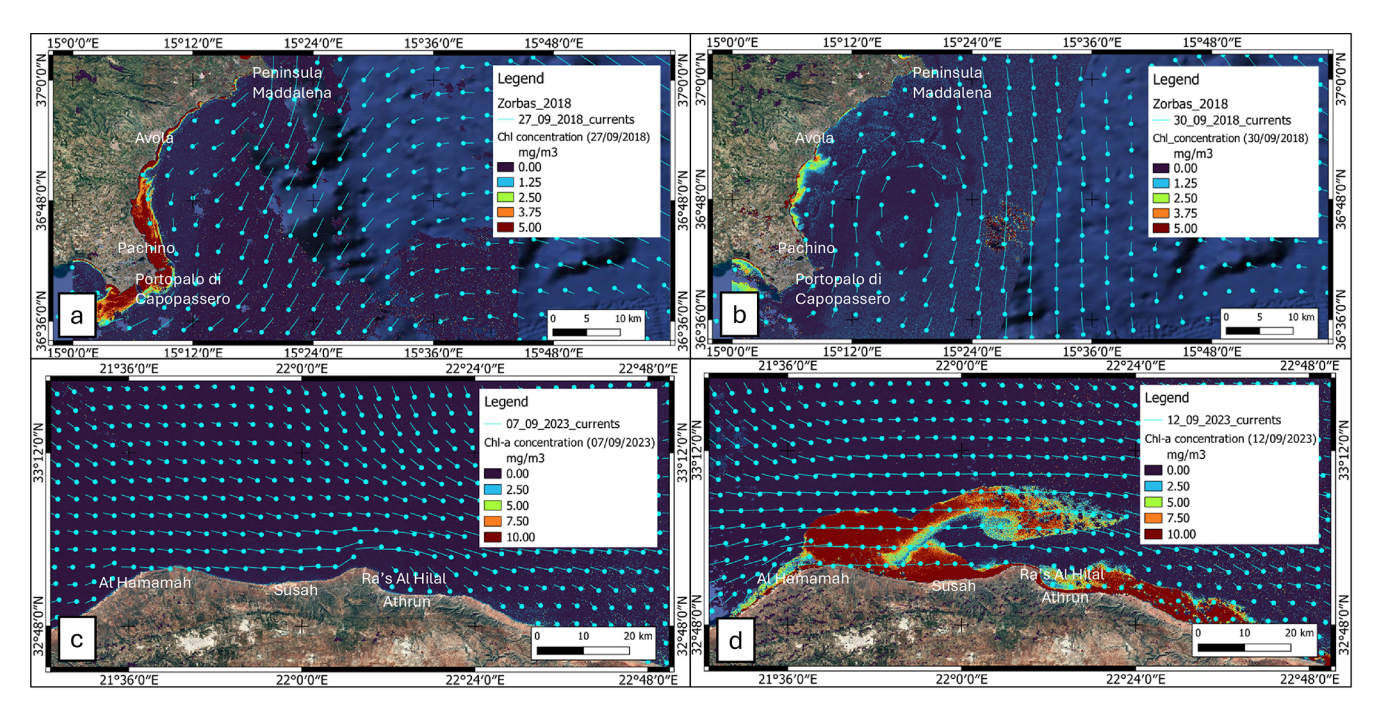


Figure 9. Surface changes of Chl *a* assessed from Sentinel 2 MSI images with current vectors derived from Copernicus reanalysis (background maps provided by © Google Earth 2023); (a) Chl *a* concentration off southeastern Sicily prior to the occurrence of medicane Zorbas (27 September 2018); (b) Chl *a* concentration after the impact of medicane Zorbas (30 September 2018); (c) Chl *a* concentration along the Libyan coasts prior to the occurrence of Daniel (7 September 2023); (d) Chl *a* concentration after the impact of Daniel (12 September 2023).

Air-sea heat exchange may also play an important role in generating eddy-induced upwelling, particularly in driving SST cooling (Liu et al., 2020; Varlas et al., 2020). Evaluation of the surface heat fluxes allowed to obtain the E_{total} lost within the sea regions impacted by the cyclones. Negative values of E_{total} indicate heat energy lost by the sea surface, which are related to air-sea interaction processes during the cyclone passage (Liu et al., 2019; Walker et al., 2005). In particular, a negative correlation was observed between E_{total} lost by sea water during the cyclone occurrence and DCM uplift (Fig. 10b). This pattern indicates that DCM uplift is strongly influenced by cooling processes occurring during intense cyclones, such as upwelling, radiative heat loss, and vertical mixing. These processes may be enhanced in the case of intense cyclones that persist in a given area for longer. However, Fig. 10c shows that, among slow-moving cyclones, the DCM uplift increases weakly with the translational speed; conversely, Fig. 10d shows that a longer lifetime is associated with a greater DCM uplift.

A decrease in the intensity of heat surface fluxes may be due to the sea surface cooling (Avolio et al., 2024; Kotta, 2023; Kotta and Kitsiou, 2019b; Scardino et al., 2024) and the consequent cyclone weakening in areas that are already influenced by upwelling; for example, Fig. 11 shows the time evolution between heat fluxes and SST in the case of Zorbas. The figure shows that the increase in fluxes induces a cooling in the SST, which feedbacks in a weakening of the fluxes

Slow-moving cyclones can enhance wind-driven up-welling through the wind pump effect (Mourre et al., 2023). In fact, according to Yang et al. (2024), while TLCs are responsible for a pronounced sea surface cooling along their track, the translation motion of a TLC could generate an inertial pumping in its lee, leading to a pattern of alternating downwelling and upwelling areas (Geisler, 1970; Shay et al., 1992; Suzuki et al., 2011; Yang et al., 2024), mainly in the cyclone peripheries (Yang et al., 2024).

Owing to the spatial distribution of wind stress, downwelling outside the cyclone's maximum radius is generally weaker than upwelling near the cyclone's centre (Fig. 12a). Therefore, a significant DCM uplift is observed near the cyclone centre related to strong upwelling currents, while the periphery and rainbands are characterized by an alternating pattern of downwelling and upwelling and weak DCM changes (Fig. 12b). Notably, when TLCs translate more rapidly, the upper ocean response – governed by Ekman dynamics – becomes weaker because the system lacks sufficient time to develop fully formed upwelling and downwelling processes (Fu et al., 2014; Liu et al., 2019).

A different behaviour was observed in the nearshore areas through the analysis of multispectral satellite images. The contribution from suspended organic matter increased the Chl *a* concentrations in the nearshore, enhanced by extreme rainfall. This occurred in response to the strong surface runoff influencing the coastal areas. However, some Mediter-

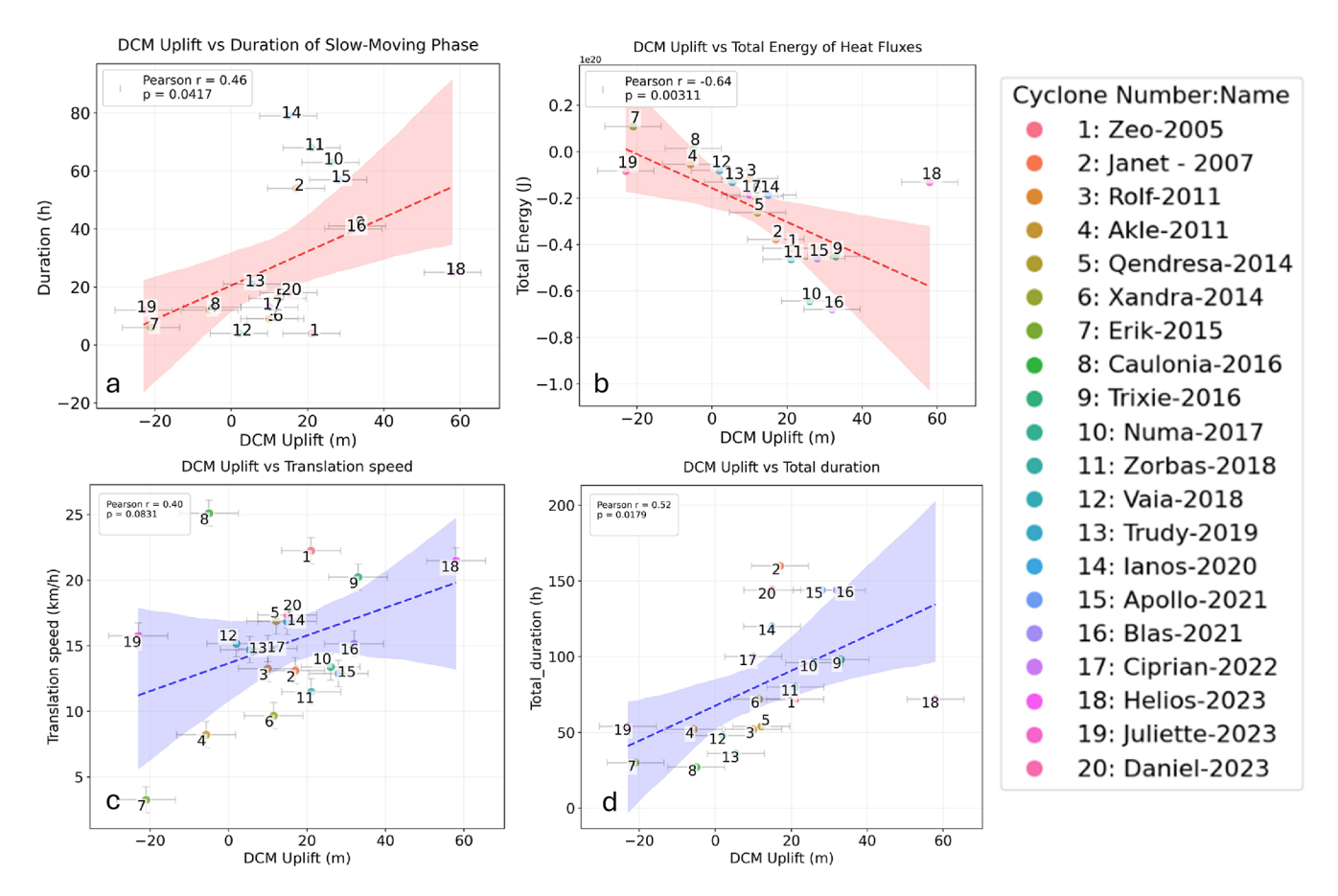


Figure 10. Correlation between DCM uplift and duration and intensity of the Mediterranean cyclones; (a) positive correlation between duration of slow-moving phases and DCM uplift; (b) negative correlation between total energy lost by sea water and DCM uplift; (c) correlation between translation speed assessed during slow-moving phase and DCM uplift; (d) positive correlation between total duration of cyclones (including no-stationary phases) and DCM uplift.

ranean hurricanes did not experience extreme rainfall in the impacted areas, as during medicane Zorbas in southeastern Sicily (Kushabaha et al., 2024; Scicchitano et al., 2021). The high Chl a concentration observed nearshore via satellite on 27 September 2018 contributed to elevated Chl a levels in offshore areas following the medicane's impact. A joint analysis of satellite-derived Chl a concentrations (30 September 2018, 1 d after medicane Zorbas) and surface current distribution revealed a significant increase in subsurface seawater Chl a. This enhancement was driven by a gyre system that transported suspended organic matter seaward (Fig. 13).

Our analysis of twenty Mediterranean cyclones reveals that the pre-storm oceanographic condition, particularly the MLD and the strength of the seasonal thermocline, is fundamental for biogeochemical response. The general pattern that emerges from a composite analysis is one of seasonal control (Menkes et al., 2016). Strong stratification during summer and early autumn typically inhibited vertical mixing, limiting nutrient uplift (D'Ortenzio and Ribera d'Alcalà, 2009; Teruzzi et al., 2021). However, slow-moving cyclones may overcome this barrier through prolonged wind-driven

upwelling and turbulent mixing, leading to significant DCM uplift (40–60 m) and Chl *a* concentration increases (Jangir et al., 2024; Kotta and Kitsiou, 2019b). The prolonged wind forcing and significant net heat loss of these cyclones provide the sustained energy required to erode the stratification, shoal the MLD, and drive significant upwelling (Lin, 2012; Menkes et al., 2016; Walker et al., 2005).

In contrast, weak stratification during late autumn and winter facilitated easier mixing, but the response was less pronounced when the pre-storm MLD was already deep or nitrate levels were low, as observed during medicane Helios (D'Adderio et al., 2023). MLD shoaling was most pronounced in areas with initially shallow or seasonally variable MLD (Ricchi et al., 2019, 2020; Vargas-Yáñez et al., 2022). For instance, medicane Apollo (October 2021) induced a 25 m MLD shoaling in the central Mediterranean, where summer stratification was transitioning (Menna et al., 2023). Two primary factors characterized the Chl *a* changes in the Mediterranean basin: (i) the nutrient limitation due to the pre-cyclone mixing, which may have already homogenized the upper water column, depleting subsurface nutrient

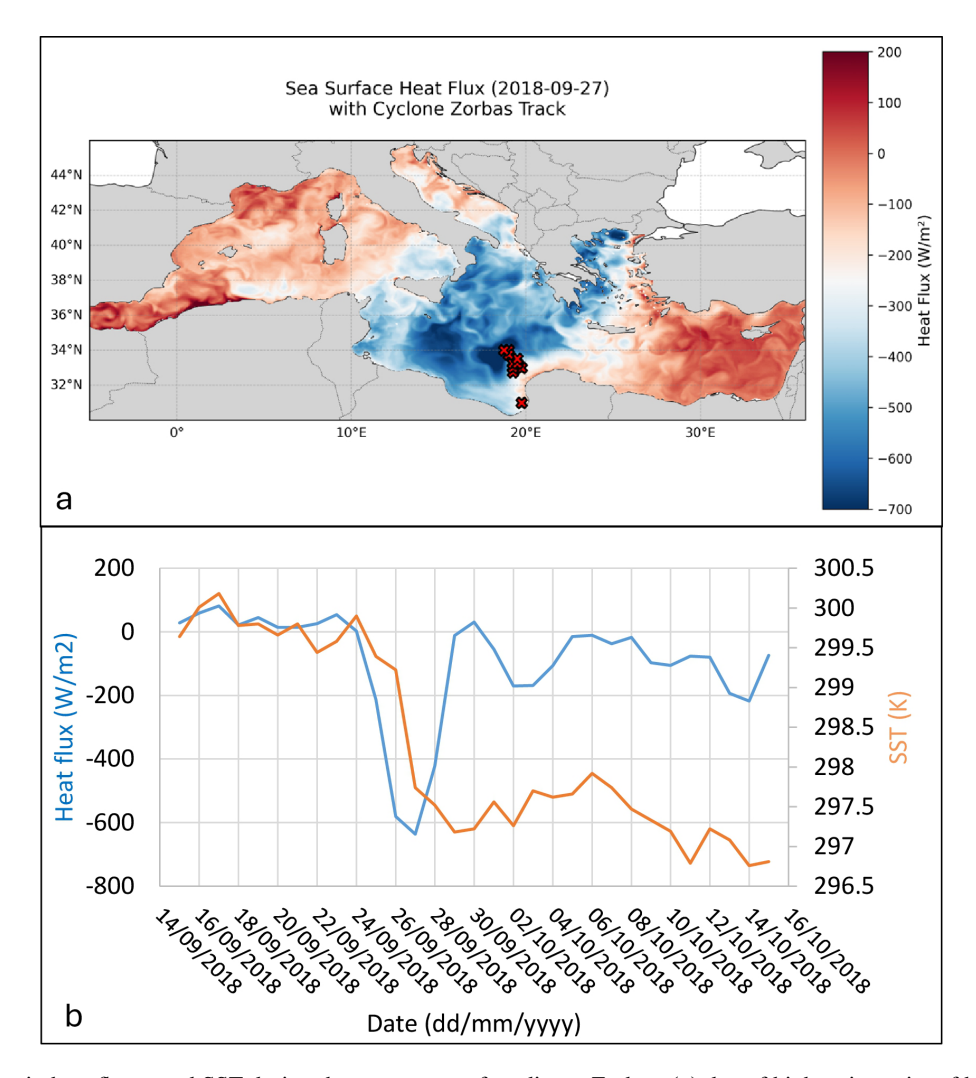


Figure 11. Decrease in heat fluxes and SST during the occurrence of medicane Zorbas; (a) day of highest intensity of heat fluxes; (b) time series of SST and surface heat fluxes extracted in the cyclogenesis location $(0.04^{\circ} \times 0.04^{\circ} \text{ grid resolution})$.

reservoirs; (ii) dilution effect due to a deep MLD, with distribution of uplifted nutrients over a larger volume.

The most substantial Chl a increases occurred in regions with abundant subsurface nitrate reservoirs, like in the Ionian Sea (Lazzari et al., 2016), particularly during slowmoving phases of medicanes like Zorbas, Apollo, and Ianos (Jangir et al., 2024; Kotta and Kitsiou, 2019b). By way of example, medicane Zorbas produced a strong biogeochemical response in the Ionian Sea, where moderate pre-storm stratification and high subsurface nitrate concentrations prevailed, but weaker effects occurred in the Peloponnese due to downwelling-favourable currents (Kassis and Varlas, 2021). Sentinel imagery also revealed an offshore transport of suspended organic matter and Chl a, evident in southeastern Sicily during medicane Zorbas (Fig. 13). Conversely, cyclone Ciprian triggered coastal upwelling near Cyprus (Fig. 14), where nitrate-rich waters enhanced the Chl a response. In contrast, weaker or faster-moving cyclones (e.g.,

Erik – 2015) had minimal effects in highly stratified or oligotrophic areas, demonstrating how pre-cyclone ocean conditions, combined with cyclone evolution, critically shape biogeochemical responses (Macías et al., 2014; Mélin et al., 2017; Menkes et al., 2016).

Conversely, other cyclones, responsible for intense rainfall, triggered intense surface runoff, which was reflected in high Chl a concentrations resembling plumes near river mouths, as observed off Libya coast following the impact of medicane Daniel in 2023 (Fig. 9d). Furthermore, a correlation between coastal upwelling and Chl a increase was also observed along the Balearic Islands during the impact of Blas (Mourre et al., 2023) and along the Cyprus coasts during the impact of Ciprian (analysis reported in Fig. 14).

Other authors reported a different behavior for other kinds of intense weather systems worldwide (Chen et al., 2017; Macías et al., 2014; Wu et al., 2007). For example, Typhoon Trami in the northwest Pacific Ocean triggered an increase

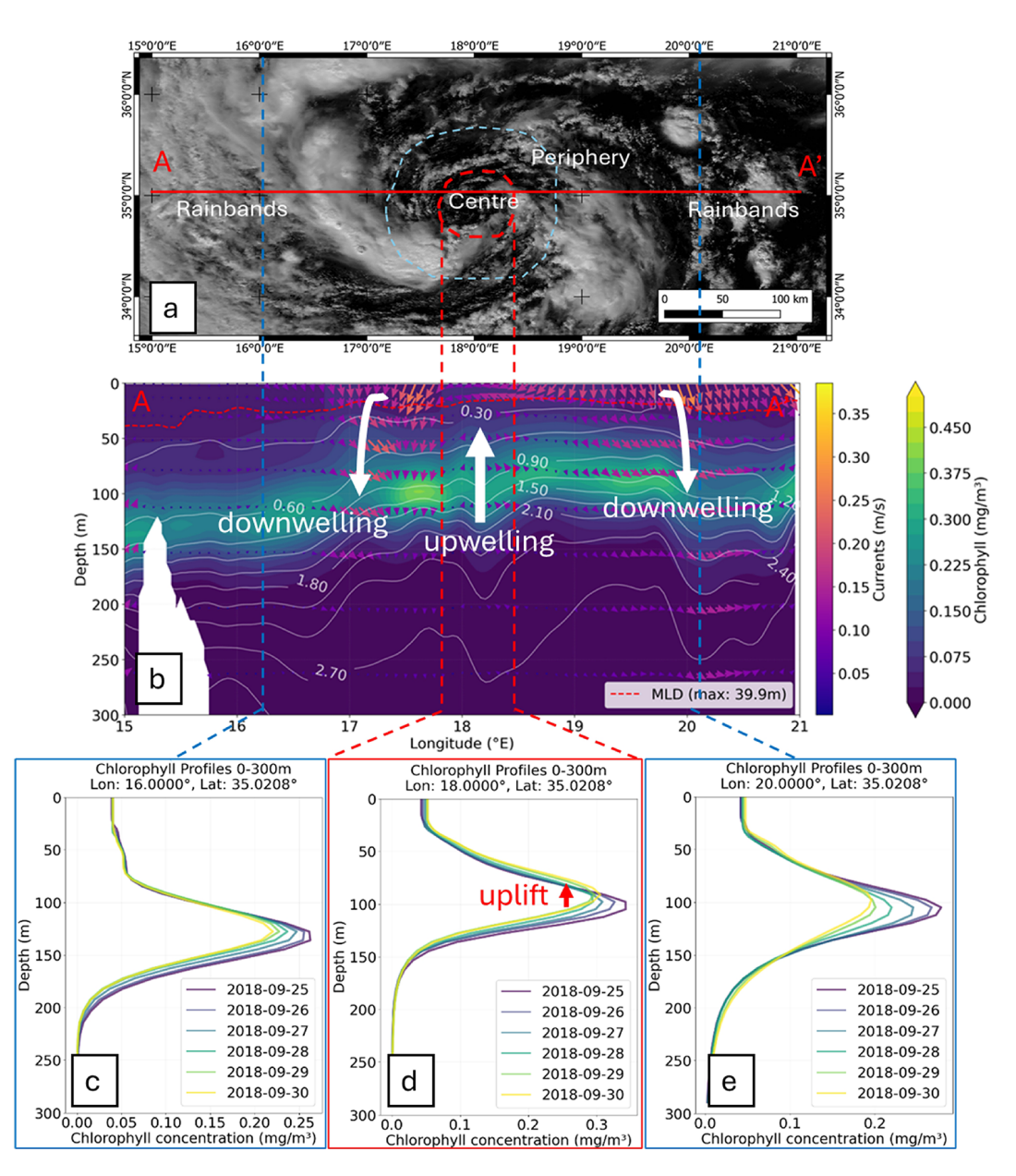


Figure 12. Features of Chl *a* changes related to the structure of the medicane Zorbas; the cyclone centre highlighted the DCM uplift and upwelling, while periphery and rainbands display alternating downwelling and upwelling; (a) satellite image of medicane Zorbas (MODIS image-acquired on 28 September 2018) highlighting the cyclone centre and periphery; (b) cross-section of biogeochemical variables referred to the time of MODIS image showing: chlorophyll *a* concentration (viridis colormap), Nitrate concentration in mmol m⁻³ (white contour lines), Current vectors (plasma-colored arrows), Mixed layer depth (MLD, red dashed line); (c-e) changes in DCM assessed from Chl *a* vertical profiles (note the DCM uplift in the cyclone centre).

of Chl *a* concentration in the surface layer related to MLD deepening, and to the consequent enrichment of the surface layer with DCM waters through mixing (Chai et al., 2021). Mediterranean cyclones induce DCM uplift through wind-driven mixing and upwelling, bringing nutrients to the euphotic zone. This aligns with observations in the Pacific and Atlantic, where cyclones enhance primary productivity via vertical mixing (Lin, 2012; Zhao et al., 2008). The dome-shaped uplift of biogeochemical variables (e.g., MLD

shoaling, nitrate enrichment) near the cyclone centre mirrors patterns seen in tropical cyclones (Price, 1981; Sanford et al., 1987; Walker et al., 2005). However, Mediterranean cyclones (especially medicanes) are smaller and shorter-lived than tropical cyclones, yet their slow movement (e.g., Zorbas: 11.5 km h⁻¹) prolongs mixing, creating localized but intense biogeochemical responses. Conversely, tropical cyclones typically cover larger areas but with faster translation speeds (e.g., 20–30 km h⁻¹; Fu et al., 2014). Mediterranean

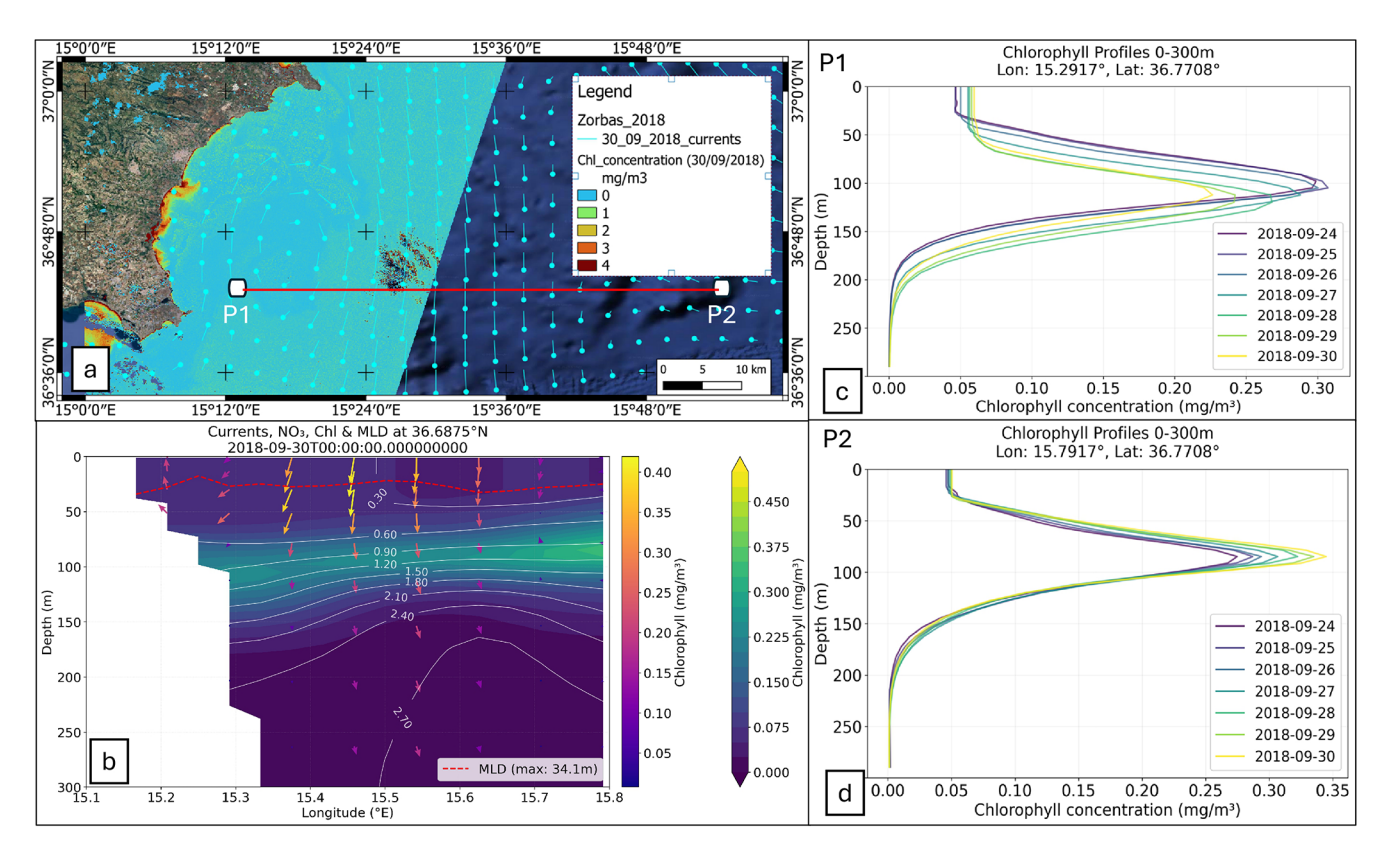


Figure 13. Dynamics of Chl *a* on the offshore and nearshore area during the impact of medicane Zorbas in southeastern Sicily; (**a**) areal Chl *a* concentration assessed through Sentinel 2 image after the impact of medicane Zorbas (background maps provided by © Google Earth 2023), red line indicates the cross-section in (**b**); (**b**) cross-section of biogeochemical variables extracted from Copernicus reanalysis products; (**c**) vertical profiles of Chl *a* changes extracted in P1; (**d**) vertical profiles of Chl *a* changes extracted in P2.

coastal upwelling (e.g., during Blas or Ciprian) is often winddriven and localized, unlike large-scale equatorial upwelling zones affected by tropical cyclones. However, the MLD in the Mediterranean Sea is highly influenced by seasonal variations and can differ significantly between summer and winter (Barboni et al., 2023; D'Ortenzio et al., 2005). The MLD depth can influence the heat fluxes and can enhance convection during TLCs (Ricchi et al., 2019, 2020). In our study, we observed MLD shoaling in areas where cyclones exhibited slow or quasi-stationary movement, while the peripheries of the cyclones were characterized by MLD deepening. This pattern can be attributed to strong upwelling in the cyclone eye (inducing MLD shoaling) and alternating downwelling and upwelling in the peripheral regions (promoting MLD deepening). The events characterized by strong vertical shear due to the water currents revealed a water mixing that enhances the MLD shoaling, as observed during medicane Trixie and cyclone Trudy (see cross-sections in the Supplement S2). As a result, the MLD may exhibit a dome-shaped structure along the tracks, as already reported for medicane Apollo (Menna et al., 2023).

The confined nature and complex coastline of the Mediterranean Sea amplify the coastal impacts of TLCs. Our anal-

ysis reveals that excluding cyclones within $100\,\mathrm{km}$ of the coast eliminates most Chl a concentrations (> $2\,\mathrm{mg\,m^{-3}}$), which are exclusively associated with terrestrial processes like runoff-driven plumes (e.g., medicane Daniel; Normand and Heggy, 2024) or the coastal resuspension and advection of organic matter (e.g., medicane Zorbas; Kotta, 2023). In contrast, the purely offshore response, though covering a larger area, yields more modest Chl a increases (0.01–0.1 $\mathrm{mg\,m^{-3}}$) driven solely by DCM uplift. This highlights that the most dramatic surface blooms are a direct product of the Mediterranean's unique biogeography (Macías et al., 2014; Marañón et al., 2021), while the subsurface offshore uplift remains a critical mechanism for enhancing nutrient cycling in the basin's oligotrophic open waters (D'Ortenzio and Ribera d'Alcalà, 2009)/

Furthermore, the Mediterranean Sea is nutrient-limited, with surface Chl *a* typically ranging from 0.05 to 0.3 mg m⁻³ (Marty and Chiavérini, 2002; Moutzouris-Sidiris and Topouzelis, 2021; Teruzzi et al., 2021). Cyclone occurrence could disrupt the water column stratification, injecting nitrate (0.5–0.8 mmol m⁻³) and phosphate into the euphotic zone (Fig. 5 and 7). This pulsed nutrient supply can be particularly significant in late summer and autumn,

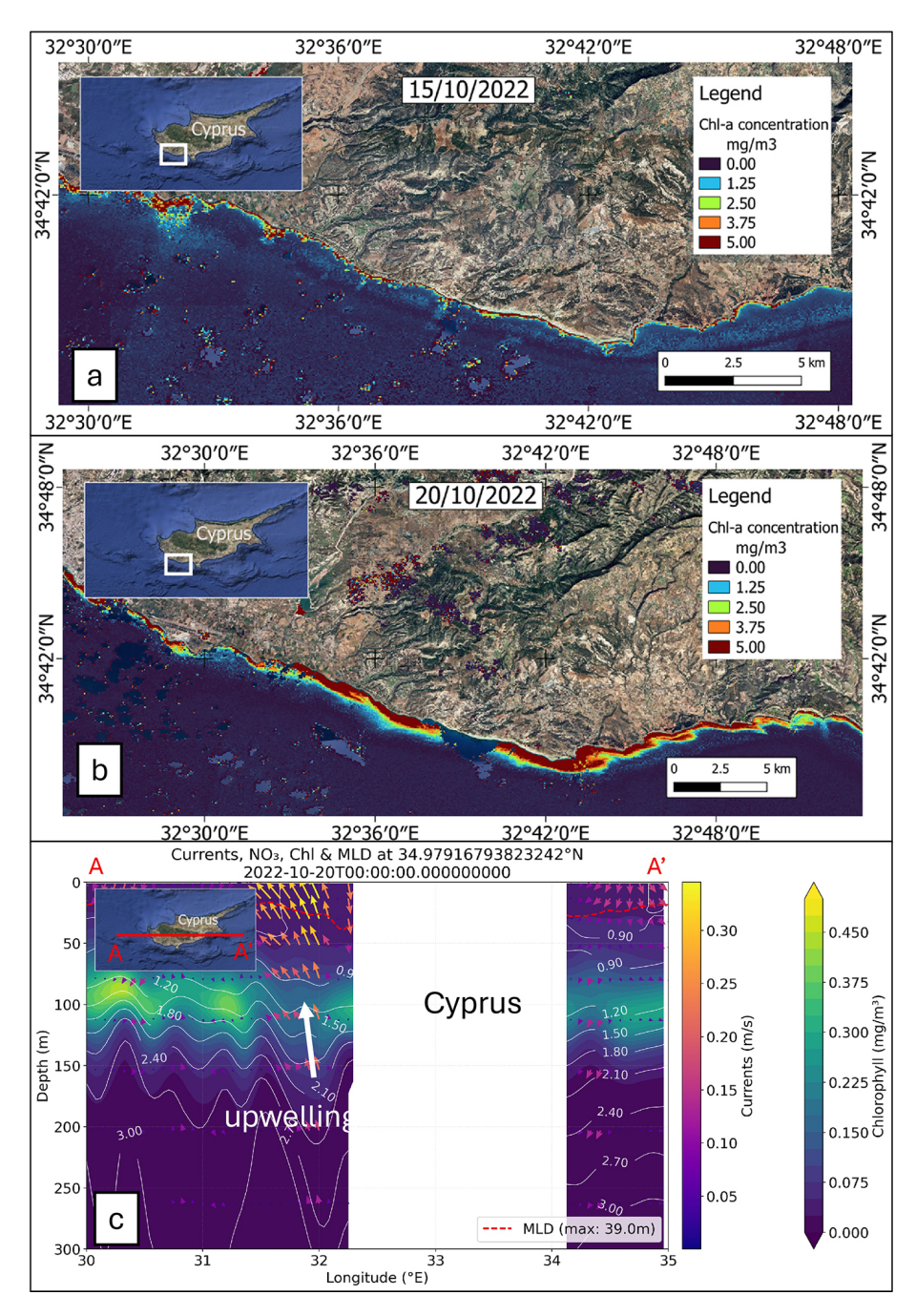


Figure 14. Coastal upwelling induced DCM uplift and increased Chl *a* concentration during the EC Ciprian (16–20 October 2022) (background maps provided by © Google Earth 2023); (a) Chl *a* assessment from Sentinel 2 images acquired on 15 October 2022 (prior of cyclone onset); (b) Chl *a* assessment from Sentinel 2 image acquired on 20 October 2022 (end of the cyclone lifetime); (c) cross-section of biogeochemical variables revealing a coastal upwelling on the western side of Cyprus island.

when the Mediterranean stratified surface waters are most nutrient-depleted (D'Ortenzio et al., 2005; D'Ortenzio and Ribera d'Alcalà, 2009). For instance, slow-moving medicanes, like Ianos (September 2020), drove 20–60 m uplifts of DCM, enhancing Chl *a* concentrations by 0.01–0.02 mg m⁻³

- comparable to the effects of seasonal riverine inputs in coastal zones (Ludwig et al., 2009).

These nutrient pulses can shift plankton community composition, favouring larger, fast-growing diatoms over smaller picoplankton that dominate under oligotrophic conditions (Marty and Chiavérini, 2002). Such shifts have been ob-

served following medicane Apollo (2021), where diatom blooms coincided with DCM shoaling (Menna et al., 2023). This transition from microbial loop-dominated recycling to a classical diatom-copepod food web can enhance carbon export efficiency (Chen et al., 2017; Cullen, 2015), potentially offsetting productivity declines associated with marine heatwaves (Androulidakis and Pytharoulis, 2025; Darmaraki et al., 2019; Izquierdo et al., 2022; Li et al., 2024a).

The cumulative impact of cyclones on annual productivity budgets is likely modest ($\leq 5\%$ -10% in affected areas), but their role in late-season nutrient injection and carbon export could grow under climate change, especially if warming SSTs intensify cyclone-driven mixing (Avolio et al., 2024; González-Alemán et al., 2019). Future studies should quantify how these event-scale perturbations integrate into broader biogeochemical cycles and whether they enhance ecosystem resilience to stratification.

5 Conclusions

This study elucidates the biogeochemical responses of the Mediterranean Sea to TLCs and ECs, with a focus on Chl *a* dynamics. Our findings highlight that slow-moving cyclones induced pronounced DCM uplift offshore, with values from 40 to 60 m. This uplift is driven by a combination of intense heat loss at the sea surface, wind-driven water mixing, intensified upwelling currents, and shoaling of the MLD, which collectively enhance nutrient availability in the euphotic zone.

The analysis revealed distinct spatial patterns in Chl *a* variability. Offshore regions along the tracks, particularly within cyclone centres, experienced significant DCM uplift due to upwelling, while peripheral areas showed alternating upwelling/downwelling currents with minimal DCM changes. This behaviour is reflected in a dome-shaped DCM along the cyclone track. Nearshore regions, influenced by surface runoff and suspended organic matter, displayed elevated Chl *a* concentrations (up to 10 mg m⁻³), often forming plumes near river mouths. These nearshore effects were further modulated by cyclone-induced rainfall and surface current dynamics.

Our results underscore the dual role of Mediterranean cyclones in shaping marine productivity: offshore, through physical mechanisms that redistribute nutrients vertically, and nearshore, through terrestrial inputs and surface transport. These insights have implications for predicting primary productivity shifts under changing cyclone regimes, particularly in the context of climate change. In this perspective, the role of cyclones in late-summer and autumn biogeochemical processes should also be investigated in the light of the inhibition of spring phytoplankton blooms by increasingly frequent and intense marine heatwaves. Future research should explore the long-term ecological impacts of these episodic events and their potential feedback on Mediterranean marine ecosystems.

Appendix A

Table A1. Intensity variables of the analysed Mediterranean cyclones derived from ERA5 reanalysis data, the translation speed is referred to average speed during the slow-movement phases.

Cyclone	Total duration (h)	$\begin{array}{c} \text{Maximum} \\ \text{wind} \\ \text{speed} \\ (\text{km h}^{-1}) \end{array}$	Minima MSLP (hPa)	Time range of slow-movement phase	Duration of slow- movement phase (h)	Translation speed (km h ⁻¹)
Zeo – 2005	72	93.5	989	13 Dec 2005 17:00:00 13 Dec 2005 21:00:00	4	22.24
Janet – 2007	160	60	1012	16 Oct 2007 15:00:00 18 Oct 2007 21:00:00	54	13.1
Rolf – 2011	52	71	996	6 Nov 2011 05:00:00/ 6 Nov 2011 14:00:00	9	13.25
Akle – 2011	52	60	1009	2 Jan 2011 10:00:00/ 2 Jan 2011 22:00:00	12	8.23
Qendresa – 2014	54	87.6	993	7 Nov 2014 18:00:00 8 Nov 2014 10:00:00	16	16.88
Xandra – 2014	72	76	990	1 Dec 2014 04:00:00 1 Dec 2014 13:00:00	9	9.68
Erik – 2015	30	55	1003	22 May 2015 00:00:00 22 May 2015 06:00:00	6	3.27
Caulonia – 2016	27	59	1011	16 Mar 2016 00:00:00 16 Mar 2016 13:00:00	13	25.1
Trixie – 2016	98	70	1012	28 Oct 2016 16:00:00 30 Oct 2016 09:00:00	41	20.23
Numa – 2017	96	66	1004	16 Nov 2017 14:00:00 19 Nov 2017 05:00:00	63	13.38
Zorbas – 2018	80	88	995	27 Sept 2018 06:00:00 30 Sep 2018 12:00:00	68	11.49
Vaia – 2018	48	100	994	28 Oct 2018 05:00:00/ 29 Oct 2018 09:00:00	4	15.16
Trudy – 2019	36	78	998	11 Nov 2019 00:00:00/ 11 Nov 2019 21:00:00	21	14.7
Ianos – 2020	120	64	1004	16 Sep 2020 11:00:00 19 Sep 2020 18:00:00	79	16.85
Apollo – 2021	144	66	1003	28 Oct 2021 23:00:00/ 31 Oct 2021 12:00:00	57	12.89
Blas – 2021	144	75	1005	10 Nov 2021 23:00:00/ 12 Nov 2021 15:00:00	40	15.14
Ciprian – 2022	100	58	1005	19 Oct 2022 05:00:00/ 19 Oct 2022 18:00:00	13	14.78
Helios —2023	72	74	1011	9 Feb 2023 23:00:00/ 11 Feb 2023 00:00:00	25	21.48
Juliette – 2023	54	80	997	28 Feb 2023 00:00:00/ 28 Feb 2023 12:00:00	12	15.75
Daniel – 2023	144	65	997.16	10 Sep 2023 11:00:00 11 Sep 2023 05:00:00	18	17.34

Data availability. The dataset generated in this study, including DCM uplift and cyclone total energy, is available at: https://doi.org/10.5281/zenodo.15912789 (Scardino et al., 2025).

Third-party repository for MSLP: ERA5: Fifth generation of ECMWF atmospheric reanalyses of the global climate. Copernicus Climate Change Service Climate Data Store (CDS): https://cds. climate.copernicus.eu/cdsapp#!/home (last access: 1 June 2025).

Third-party repository for biogeochemical variables: Cossarini et al. (2021).

Third-party repository for currents and MLD:

https://doi.org/

(Escudier et al., 2020;

https://doi.org/

2. 10.25423/cmcc/medsea_analysis_forecast_phy_006_013_eas4 (Clementi et al., 2019).

Third-party direct repository for observation: https://doi.org/10.17882/42182 (Argo, 2023).

Supplement. The supplement related to this article is available online at https://doi.org/10.5194/os-21-2849-2025-supplement.

Author contributions. GSca and AK wrote the main text, analysed climate datasets and processed the Chl a concetration from reanalysis and remote sensing data. MMM and DB revised the concept related to the slow-moving phases and intensity of Mediterranean cyclones and provided a revised version of the manuscript. GSca, MMM, and GSci reported a validation on the model outputs. GSci performed the supervision and investigation and provided the resources for the research.

Disclaimer. Publisher's note: Copernicus Publications remains neutral with regard to jurisdictional claims made in the text, published maps, institutional affiliations, or any other geographical representation in this paper. While Copernicus Publications makes every effort to include appropriate place names, the final responsibility lies with the authors. Views expressed in the text are those of the authors and do not necessarily reflect the views of the publisher.

Acknowledgements. This work has greatly benefited from contributions of the ERC SEED UNIBA project "Get aHead Of the MEdicanes: strategies for the COASTal environment - HOME-COAST" (Principal Investigator Giovanni Scardino, PhD). The validation methods for the Sentinel-2 and Sentinel-3 dataset were supported by the Sentinel-3 Validation Team (S3VT) under the project "Frozen Coasts under Climate Change" (Principal Investigator Giovanni Scardino, PhD, ESA project PP0092792). This paper and related research have been conducted within the framework of the Italian inter-university PhD course in sustainable development and climate change (link: https://www.phd-sdc.it/, last access: 1 July 2025) "Medichange" (responsible Giovanni Scicchitano). This work was partly supported by the European Space Agency through the CYMS project (Contract 4000129822/19/I-DT - https://www.esa-cyms.org/, last access: 8 July 2025), "Earth observations as a cornerstone to the understanding and prediction of tropical-like cyclone risk in the Mediterranean (MEDICANES)," and ESA Contract 4000144111/23/I-KE. MMM also acknowledges financial support from Next Generation EU, mission 4, component 1, CUP B53D23007360006, Project "WIND RISK".

Competing interests. The contact author has declared that none of the authors has any competing interests.

1. 10.25423/CMCC/MEDSEA_MULTIYEAR_PHY_006_004_E3R1 Financial support. This research has been funded by the PRIN 2022 PNRR project titled "ARCHIMEDE - Multidisciplinary approach to better define vulnerability and hazard of Medicanes along the Ionian coasts of Sicily" (CUP H53D23011380001, Principal Investigator Giovanni Scicchitano).

> Review statement. This paper was edited by Mario Hoppema and reviewed by two anonymous referees.

References

Androulidakis, Y. and Pytharoulis, I.: Variability of marine heatwaves and atmospheric cyclones in the Mediterranean Sea during the last four decades, Environ. Res. Lett., 20, 034031, https://doi.org/10.1088/1748-9326/adb505, 2025.

Argo: Argo float data and metadata from the Global Data Assembly Centre (GDAC), SEANOE [data set], https://doi.org/10.17882/42182, 2023.

Argüeso, D., Marcos, M., and Amores, A.: Storm Daniel fueled by anomalously high sea surface temperatures in the Mediterranean, npj Clim. Atmos. Sci., 7, 1-12, https://doi.org/10.1038/s41612-024-00872-2, 2024.

Athanasiou, P., van Dongeren, A., Giardino, A., Vousdoukas, M., Gaytan-Aguilar, S., and Ranasinghe, R.: Global distribution of nearshore slopes with implications for coastal retreat, Earth Syst. Sci. Data, 11, 1515-1529, https://doi.org/10.5194/essd-11-1515-2019, 2019.

Avolio, E., Fanelli, C., Pisano, A., and Miglietta, M. M.: Unveiling the Relationship Between Mediterranean Tropical-Like Cyclones and Rising Sea Surface Temperature, Geophys. Res. Lett., 51, e2024GL109921, https://doi.org/10.1029/2024GL109921, 2024.

Barboni, A., Coadou-Chaventon, S., Stegner, A., Le Vu, B., and Dumas, F.: How subsurface and double-core anticyclones intensify the winter mixed-layer deepening in the Mediterranean Sea, Ocean Sci., 19, 229-250, https://doi.org/10.5194/os-19-229-2023, 2023.

Belkin, I. M.: Rapid warming of Large Marine Ecosystems, Prog. Oceanogr., 81. 207-213. https://doi.org/10.1016/j.pocean.2009.04.011, 2009.

Carrió, D. S.: Improving the predictability of the Qendresa Medicane by the assimilation of conventional and atmospheric motion vector observations. Storm-scale analysis and shortrange forecast, Nat. Hazards Earth Syst. Sci., 23, 847-869, https://doi.org/10.5194/nhess-23-847-2023, 2023.

- Cavicchia, L., von Storch, H., and Gualdi, S.: Mediterranean Tropical-Like Cyclones in Present and Future Climate, J. Climate, 27, 7493–7501, https://doi.org/10.1175/JCLI-D-14-00339.1, 2014.
- Chai, F., Wang, Y., Xing, X., Yan, Y., Xue, H., Wells, M., and Boss, E.: A limited effect of sub-tropical typhoons on phytoplankton dynamics, Biogeosciences, 18, 849–859, https://doi.org/10.5194/bg-18-849-2021, 2021.
- Chen, D., He, L., Liu, F., and Yin, K.: Effects of typhoon events on chlorophyll and carbon fixation in different regions of the East China Sea, Estuar. Coast. Shelf Sci., 194, 229–239, https://doi.org/10.1016/j.ecss.2017.06.026, 2017.
- Clementi, E., Pistoia, Escudier, R., Delrosso, D., Drudi, M., Grandi, A., Lecci, R., Cretí, S., Ciliberti, S., Coppini, G., Masina, S., and Pinardi, N.: Mediterranean Sea Physical Analysis and Forecast (CMEMS MED-Currents 2016–2019), CMEMS Copernicus Monitoring Environment Marine Service [data set], https://doi.org/10.25423/cmcc/medsea_analysis_forecast_phy, 2010
- Comellas Prat, A., Federico, S., Torcasio, R. C., D'Adderio, L. P., Dietrich, S., and Panegrossi, G.: Evaluation of the Sensitivity of Medicane Ianos to Model Microphysics and Initial Conditions Using Satellite Measurements, Remote Sens., 13, 4984, https://doi.org/10.3390/rs13244984, 2021.
- Cossarini, G., Feudale, L., Teruzzi, A., Bolzon, G., Coidessa, G., Solidoro, C., Di Biagio, V., Amadio, C., Lazzari, P., Brosich, A., and Salon, S.: High-Resolution Reanalysis of the Mediterranean Sea Biogeochemistry (1999–2019), Front. Mar. Sci., 8, https://doi.org/10.3389/fmars.2021.741486, 2021.
- Cullen, J. J.: Subsurface chlorophyll maximum layers: enduring enigma or mystery solved?, Ann. Rev. Mar. Sci., 7, 207–239, https://doi.org/10.1146/annurev-marine-010213-135111, 2015.
- D'Adderio, L. P., Casella, D., Dietrich, S., Sanò, P., and Panegrossi, G.: GPM-CO observations of Medicane Ianos: Comparative analysis of precipitation structure between development and mature phase, Atmos. Res., 273, 106174, https://doi.org/10.1016/j.atmosres.2022.106174, 2022.
- D'Adderio, L. P., Panegrossi, G., Dafis, S., Rysman, J.-F., Casella, D., Sanò, P., Fuccello, A., and Miglietta, M. M.: Helios and Juliette: Two Falsely Acclaimed Medicanes, SSRN, https://doi.org/10.2139/ssrn.4542818, 2023.
- Dafis, S., Claud, C., Kotroni, V., Lagouvardos, K., and Rysman, J.-F.: Insights into the convective evolution of Mediterranean tropical-like cyclones, Q. J. Roy. Meteorol. Soc., 146, 4147– 4169, https://doi.org/10.1002/qj.3896, 2020.
- Darmaraki, S., Somot, S., Sevault, F., Nabat, P., Cabos Narvaez, W. D., Cavicchia, L., Djurdjevic, V., Li, L., Sannino, G., and Sein, D. V.: Future evolution of Marine Heatwaves in the Mediterranean Sea, Clim. Dynam., 53, 1371–1392, https://doi.org/10.1007/s00382-019-04661-z, 2019.
- Davolio, S., Fera, S. D., Laviola, S., Miglietta, M. M., and Levizzani, V.: Heavy Precipitation over Italy from the Mediterranean Storm "Vaia" in October 2018: Assessing the Role of an Atmospheric River, Mon. Weather Rev., 148, 3571–3588, https://doi.org/10.1175/MWR-D-20-0021.1, 2020.
- de la Vara, A., Gutiérrez-Fernández, J., González-Alemán, J. J., and Gaertner, M. Á.: Characterization of medicanes with a minimal number of geopotential levels, Int. J. Climatol., 41, 3300–3316, https://doi.org/10.1002/joc.7020, 2021.

- Di Francesca, V., D'Adderio, L. P., Sanò, P., Rysman, J.-F., Casella, D., and Panegrossi, G.: Passive microwave-based diagnostics of medicanes over the period 2000–2021, Atmos. Res., 316, 107922, https://doi.org/10.1016/j.atmosres.2025.107922, 2025.
- Di Muzio, E., Riemer, M., Fink, A. H., and Maier-Gerber, M.: Assessing the predictability of Medicanes in ECMWF ensemble forecasts using an object-based approach, Q. J. Roy. Meteorol. Soc., 145, 1202–1217, https://doi.org/10.1002/qj.3489, 2019.
- D'Ortenzio, F. and Ribera d'Alcalà, M.: On the trophic regimes of the Mediterranean Sea: a satellite analysis, Biogeosciences, 6, 139–148, https://doi.org/10.5194/bg-6-139-2009, 2009.
- D'Ortenzio, F., Iudicone, D., de Boyer Montegut, C., Testor, P., Antoine, D., Marullo, S., Santoleri, R., and Madec, G.: Seasonal variability of the mixed layer depth in the Mediterranean Sea as derived from in situ profiles, Geophys. Res. Lett., 32, https://doi.org/10.1029/2005GL022463, 2005.
- Escudier, R., Clementi, E., Omar, M., Cipollone, A., Pistoia, J., Aydogdu, A., Drudi, M., Grandi, A., Lyubartsev, V., Lecci, R., Cretí, S., Masina, S., Coppini, G., and Pinardi, N.: Mediterranean Sea Physical Reanalysis (CMEMS MED-Currents) (Version 1) Data set, CMEMS Copernicus Monitoring Environment Marine Service [data set], https://doi.org/10.25423/CMCC/MEDSEA_MULTIYEAR_PHY, 2020.
- Federico, S., Comellas Prat, A., Torcasio, R. C., D'Adderio, L. P., Dietrich, S., and Panegrossi, G.: Medicane Ianos: a comparative study between WRF model and satellite measurements, EMS Annual Meeting 2021, online, 6–10 Sep 2021, EMS2021-297, https://doi.org/10.5194/ems2021-297, 2021.
- Fita, L., Romero, R., Luque, A., Emanuel, K., and Ramis, C.: Analysis of the environments of seven Mediterranean tropical-like storms using an axisymmetric, nonhydrostatic, cloud resolving model, Nat. Hazards Earth Syst. Sci., 7, 41–56, https://doi.org/10.5194/nhess-7-41-2007, 2007.
- Flaounas, E., Davolio, S., Raveh-Rubin, S., Pantillon, F., Miglietta, M. M., Gaertner, M. A., Hatzaki, M., Homar, V., Khodayar, S., Korres, G., Kotroni, V., Kushta, J., Reale, M., and Ricard, D.: Mediterranean cyclones: current knowledge and open questions on dynamics, prediction, climatology and impacts, Weather Clim. Dynam., 3, 173–208, https://doi.org/10.5194/wcd-3-173-2022, 2022.
- Flaounas, E., Aragão, L., Bernini, L., Dafis, S., Doiteau, B., Flocas, H., Gray, S. L., Karwat, A., Kouroutzoglou, J., Lionello, P., Miglietta, M. M., Pantillon, F., Pasquero, C., Patlakas, P., Picornell, M. Á., Porcù, F., Priestley, M. D. K., Reale, M., Roberts, M. J., Saaroni, H., Sandler, D., Scoccimarro, E., Sprenger, M., and Ziv, B.: A composite approach to produce reference datasets for extratropical cyclone tracks: application to Mediterranean cyclones, Weather Clim. Dynam., 4, 639–661, https://doi.org/10.5194/wcd-4-639-2023, 2023.
- Flaounas, E., Dafis, S., Davolio, S., Faranda, D., Ferrarin, C., Hartmuth, K., Hochman, A., Koutroulis, A., Khodayar, S., Miglietta, M. M., Pantillon, F., Patlakas, P., Sprenger, M., and Thurnherr, I.: Dynamics, predictability, impacts, and climate change considerations of the catastrophic Mediterranean Storm Daniel (2023), EGUsphere [preprint], https://doi.org/10.5194/egusphere-2024-2809, 2024.
- Fu, H., Wang, X., Chu, P. C., Zhang, X., Han, G., and Li, W.: Tropical cyclone footprint in the ocean mixed layer observed by Argo

- in the Northwest Pacific, J. Geophys. Res.-Oceans, 119, 8078–8092, https://doi.org/10.1002/2014JC010316, 2014.
- Gallisai, R., Volpe, G., and Peters, F.: Large Saharan dust storms: Implications for chlorophyll dynamics in the Mediterranean Sea, Global Biogeochem. Cy., 30, 1725–1737, https://doi.org/10.1002/2016GB005404, 2016.
- GEBCO: The General Bathymetric Chart of the Oceans, https://www.gebco.net/ (last access: 15 April 2020), 2020.
- Geisler, J. E.: Linear theory of the response of a two layer ocean to a moving hurricane, Geophys. Fluid Dynam., 1, 249–272, https://doi.org/10.1080/03091927009365774, 1970.
- Giovannini, L., Davolio, S., Zaramella, M., Zardi, D., and Borga, M.: Multi-model convection-resolving simulations of the October 2018 Vaia storm over Northeastern Italy, Atmos. Res., 253, 105455, https://doi.org/10.1016/j.atmosres.2021.105455, 2021.
- González-Alemán, J. J., Pascale, S., Gutierrez-Fernandez, J., Murakami, H., Gaertner, M. A., and Vecchi, G. A.: Potential Increase in Hazard From Mediterranean Hurricane Activity With Global Warming, Geophys. Res. Lett., 46, 1754–1764, https://doi.org/10.1029/2018GL081253, 2019.
- Gutiérrez-Fernández, J., Miglietta, M. M., González-Alemán, J. J., and Gaertner, M. A.: A New Refinement of Mediterranean Tropical-Like Cyclones Characteristics, Geophys. Res. Lett., 51, e2023GL106429, https://doi.org/10.1029/2023GL106429, 2024.
- Izquierdo, P., Taboada, F. G., González-Gil, R., Arrontes, J., and Rico, J. M.: Alongshore upwelling modulates the intensity of marine heatwaves in a temperate coastal sea, Sci. Total Environ., 835, 155478, https://doi.org/10.1016/j.scitotenv.2022.155478, 2022.
- Jangir, B., Mishra, A. K., and Strobach, E.: Effects of Mesoscale Eddies on the Intensity of Cyclones in the Mediterranean Sea, J. Geophys. Res.-Atmos., 128, e2023JD038607, https://doi.org/10.1029/2023JD038607, 2023.
- Jangir, B., Mishra, A. K., and Strobach, E.: The interplay between medicanes and the Mediterranean Sea in the presence of sea surface temperature anomalies, Atmos. Res., 310, 107625, https://doi.org/10.1016/j.atmosres.2024.107625, 2024.
- Karagiorgos, J., Samos, I., Vervatis, V., Sofianos, S., and Flocas, H.: The Impact of Ocean–Atmosphere Coupling on the Prediction of Mediterranean Cyclones: A Case Study of Medicane Ianos, Environ. Sci. Proceed., 26, 60, https://doi.org/10.3390/environsciproc2023026060, 2023.
- Kassis, D. and Varlas, G.: Hydrographic effects of an intense "medicane" over the central-eastern Mediterranean Sea in 2018, Dynam. Atmos. Oceans, 93, 101185, https://doi.org/10.1016/j.dynatmoce.2020.101185, 2021.
- Katara, I., Illian, J., Pierce, G., Scott, B., and Wang, J.: Atmospheric forcing on chlorophyll concentration in the Mediterranean, Hydrobiologia, 612, 33–48, https://doi.org/10.1007/s10750-008-9492-z, 2008.
- Kotta, D.: Extreme Weather Affecting Sea Chlorophyll: The Case of a Medicane, Environ. Sci. Proceed., 26, 192, https://doi.org/10.3390/environsciproc2023026192, 2023.
- Kotta, D. and Kitsiou, D.: Chlorophyll in the Eastern Mediterranean Sea: Correlations with Environmental Factors and Trends, Environments, 6, 98, https://doi.org/10.3390/environments6080098, 2019a.

- Kotta, D. and Kitsiou, D.: Medicanes Triggering Chlorophyll Increase, J. Mar. Sci. Eng., 7, 75, https://doi.org/10.3390/jmse7030075, 2019b.
- Kotta, D., Kitsiou, D., and Kassomenos, P.: First Rains as Extreme Events Influencing Marine Primary Production, Springer, 263–270, https://doi.org/10.1007/978-3-319-35095-0_37, 2017.
- Kushabaha, A., Scardino, G., Sabato, G., Miglietta, M. M.,
 Flaounas, E., Monforte, P., Marsico, A., De Santis, V., Borzì, A.
 M., and Scicchitano, G.: ARCHIMEDE An Innovative Web-GIS Platform for the Study of Medicanes, Remote Sens., 16, 2552, https://doi.org/10.3390/rs16142552, 2024.
- Lagouvardos, K., Karagiannidis, A., Dafis, S., Kalimeris, A., and Kotroni, V.: Ianos A Hurricane in the Mediterranean, B. Am. Meteorol. Soc., 103, E1621–E1636, https://doi.org/10.1175/BAMS-D-20-0274.1, 2022.
- Latha, T. P., Rao, K. H., Nagamani, P. V., Amminedu, E., Choudhury, S. B., Dutt, C. B. S., and Dadhwal, V. K.: Impact of Cyclone PHAILIN on Chlorophyll-a Concentration and Productivity in the Bay of Bengal, Int. J. Geosci., 6, 473–480, https://doi.org/10.4236/ijg.2015.65037, 2015.
- Lazzari, P., Solidoro, C., Salon, S., and Bolzon, G.: Spatial variability of phosphate and nitrate in the Mediterranean Sea: A modeling approach, Deep-Sea Res. Pt. I, 108, 39–52, https://doi.org/10.1016/j.dsr.2015.12.006, 2016.
- Li, M., Organelli, E., Serva, F., Bellacicco, M., Landolfi, A., Pisano, A., Marullo, S., Shen, F., Mignot, A., van Gennip, S., and Santoleri, R.: Phytoplankton Spring Bloom Inhibited by Marine Heatwaves in the North-Western Mediterranean Sea, Geophys. Res. Lett., 51, e2024GL109141, https://doi.org/10.1029/2024GL109141, 2024a.
- Li, X., Zheng, H., Mao, Z., Du, P., and Zhang, W.: Change in water column total chlorophyll *a* in the Mediterranean revealed by satellite observation, Sci. Total Environ., 945, 174076, https://doi.org/10.1016/j.scitotenv.2024.174076, 2024b.
- Lin, I.-I.: Typhoon-induced phytoplankton blooms and primary productivity increase in the Western North Pacific Subtropical Ocean, J. Geophys. Res.-Oceans, 117, 3039, https://doi.org/10.1029/2011JC007626, 2012.
- Listowski, C., Forestier, E., Dafis, S., Farges, T., De Carlo, M., Grimaldi, F., Le Pichon, A., Vergoz, J., Heinrich, P., and Claud, C.: Remote Monitoring of Mediterranean Hurricanes Using Infrasound, Remote Sens., 14, 6162, https://doi.org/10.3390/rs14236162, 2022.
- Liu, X., Wei, J., Zhang, D.-L., and Miller, W.: Parameterizing Sea Surface Temperature Cooling Induced by Tropical Cyclones: 1. Theory and An Application to Typhoon Matsa (2005), J. Geophys. Res.-Oceans, 124, 1215–1231, https://doi.org/10.1029/2018JC014117, 2019.
- Liu, Y., Tang, D., Tang, S., Morozov, E., Liang, W., and Sui, Y.: A case study of Chlorophyll a response to tropical cyclone Wind Pump considering Kuroshio invasion and air–sea heat exchange, Sci. Total Environ., 741, 140290, https://doi.org/10.1016/j.scitotenv.2020.140290, 2020.
- Ludwig, W., Dumont, E., Meybeck, M., and Heussner, S.: River discharges of water and nutrients to the Mediterranean and Black Sea: Major drivers for ecosystem changes during past and future decades?, Prog. Oceanogr., 80, 199–217, https://doi.org/10.1016/j.pocean.2009.02.001, 2009.

- Macías, D., Stips, A., and Garcia-Gorriz, E.: The relevance of deep chlorophyll maximum in the open Mediterranean Sea evaluated through 3D hydrodynamic-biogeochemical coupled simulations, Ecol. Model., 281, 26–37, https://doi.org/10.1016/j.ecolmodel.2014.03.002, 2014.
- Marañón, E., Van Wambeke, F., Uitz, J., Boss, E. S., Dimier, C., Dinasquet, J., Engel, A., Haëntjens, N., Pérez-Lorenzo, M., Taillandier, V., and Zäncker, B.: Deep maxima of phytoplankton biomass, primary production and bacterial production in the Mediterranean Sea, Biogeosciences, 18, 1749–1767, https://doi.org/10.5194/bg-18-1749-2021, 2021.
- Marra, A. C., Federico, S., Montopoli, M., Avolio, E., Baldini, L., Casella, D., D'Adderio, L. P., Dietrich, S., Sanò, P., Torcasio, R. C., and Panegrossi, G.: The Precipitation Structure of the Mediterranean Tropical-Like Cyclone Numa: Analysis of GPM Observations and Numerical Weather Prediction Model Simulations, Remote Sens., 11, 1690, https://doi.org/10.3390/rs11141690, 2019.
- Marty, J.-C. and Chiavérini, J.: Seasonal and interannual variations in phytoplankton production at DYFAMED time-series station, northwestern Mediterranean Sea, Deep-Sea Res. Pt. II, 49, 2017–2030, https://doi.org/10.1016/S0967-0645(02)00025-5, 2002.
- Marty, J. C. and Chiavérini, J.: Hydrological changes in the Ligurian Sea (NW Mediterranean, DYFAMED site) during 1995–2007 and biogeochemical consequences, Biogeosciences, 7, 2117–2128, https://doi.org/10.5194/bg-7-2117-2010, 2010.
- Mei, W., Lien, C.-C., Lin, I.-I., and Xie, S.-P.: Tropical Cyclone-Induced Ocean Response: A Comparative Study of the South China Sea and Tropical Northwest Pacific, J. Climate, 28, 5952– 5968, https://doi.org/10.1175/JCLI-D-14-00651.1, 2015.
- Mélin, F., Vantrepotte, V., Chuprin, A., Grant, M., Jackson, T., and Sathyendranath, S.: Assessing the fitness-for-purpose of satellite multi-mission ocean color climate data records: A protocol applied to OC-CCI chlorophyll-*a* data, Remote Sens. Environ., 203, 139–151, https://doi.org/10.1016/j.rse.2017.03.039, 2017.
- Menkes, C. E., Lengaigne, M., Lévy, M., Ethé, C., Bopp, L., Aumont, O., Vincent, E., Vialard, J., and Jullien, S.: Global impact of tropical cyclones on primary production, Global Biogeochem. Cy., 30, 767–786, https://doi.org/10.1002/2015GB005214, 2016.
- Menna, M., Martellucci, R., Reale, M., Cossarini, G., Salon, S., Notarstefano, G., Mauri, E., Poulain, P.-M., Gallo, A., and Solidoro, C.: A case study of impacts of an extreme weather system on the Mediterranean Sea circulation features: Medicane Apollo (2021), Sci. Rep., 13, 3870, https://doi.org/10.1038/s41598-023-29942-w, 2023.
- Miglietta, M. M.: Mediterranean Tropical-Like Cyclones (Medicanes), Atmosphere, 10, 206, https://doi.org/10.3390/atmos10040206, 2019.
- Miglietta, M. M. and Rotunno, R.: Development mechanisms for Mediterranean tropical-like cyclones (medicanes), Q. J. Roy. Meteorol. Soc., 145, 1444–1460, https://doi.org/10.1002/qj.3503, 2019.
- Miglietta, M. M., González-Alemán, J., Panegrossi, G., Gaertner, M., Pantillon, F., Pasquero, C., Schultz, D., D'Adderio, L. P., Dafis, S., Husson, L., Ricchi, A., Carrió, D. S., Davolio, S., Fita, L., Picornell, M. A., Pytharoulis, I., Raveh-Rubin, S., Scoccimarro, E., Bernini, L., Cavicchia, L., Conte, D., Ferretti, R., Flocas, H. A., Gutiérrez-Fernández, J., Hatzaki, M., Homar Santaner, V., Jansà, A., Patlakas, P., and Flaounas, E.: Defining

- Medicanes: Bridging the Knowledge Gap Between Tropical and Extratropical Cyclones in the Mediterranean, B. Am. Meteorol. Soc., E1955–E1971, https://doi.org/10.1175/BAMS-D-24-0289.1, 2025.
- Mignot, A., D'Ortenzio, F., Taillandier, V., Cossarini, G., and Salon, S.: Quantifying Observational Errors in Biogeochemical-Argo Oxygen, Nitrate, and Chlorophyll *a* Concentrations, Geophys. Res. Lett., 46, 4330–4337, https://doi.org/10.1029/2018GL080541, 2019.
- Mourre, B., Reyes, E., Lorente, P., Santana, A., Hernández-Lasheras, J., Hernández-Carrasco, I., García-Jove, M., and Zarokanellos, N. D.: Intense wind-driven coastal upwelling in the Balearic Islands in response to Storm Blas (November 2021), in: 7th edition of the Copernicus Ocean State Report (OSR7), edited by: von Schuckmann, K., Moreira, L., Le Traon, P.-Y., Grégoire, M., Marcos, M., Staneva, J., Brasseur, P., Garric, G., Lionello, P., Karstensen, J., and Neukermans, G., Copernicus Publications, State Planet, 1-osr7, 15, https://doi.org/10.5194/sp-1-osr7-15-2023, 2023.
- Moutzouris-Sidiris, I. and Topouzelis, K.: Assessment of Chlorophyll-*a* concentration from Sentinel-3 satellite images at the Mediterranean Sea using CMEMS open source in situ data, Open Geosci., 13, 85–97, https://doi.org/10.1515/geo-2020-0204, 2021.
- Normand, J. C. L. and Heggy, E.: Assessing flash flood erosion following storm Daniel in Libya, Nat. Commun., 15, 6493, https://doi.org/10.1038/s41467-024-49699-8, 2024.
- Owen, L. E., Catto, J. L., Stephenson, D. B., and Dunstone, N. J.: Compound precipitation and wind extremes over Europe and their relationship to extratropical cyclones, Weather Clim. Ext., 33, 100342, https://doi.org/10.1016/j.wace.2021.100342, 2021.
- Panegrossi, G., D'Adderio, L. P., Dafis, S., Rysman, J.-F., Casella, D., Dietrich, S., and Sanò, P.: Warm Core and Deep Convection in Medicanes: A Passive Microwave-Based Investigation, Remote Sens., 15, 2838, https://doi.org/10.3390/rs15112838, 2023.
- Piontkovski, S. and Al-Hashmi, K.: Atmospheric cyclones and seasonal cycles of biological productivity of the ocean, Int. J. Environ. Stud., 71, https://doi.org/10.1080/00207233.2014.880997, 2014
- Price, J. F.: Upper Ocean Response to a Hurricane, J. Phys. Oceanogr., 11, 153–175, https://doi.org/10.1175/1520-0485(1981)011<0153:UORTAH>2.0.CO;2, 1981.
- Pytharoulis, I.: Analysis of a Mediterranean tropical-like cyclone and its sensitivity to the sea surface temperatures, Atmos. Res., 208, 167–179, https://doi.org/10.1016/j.atmosres.2017.08.009, 2018.
- Ricchi, A., Miglietta, M. M., Barbariol, F., Benetazzo, A., Bergamasco, A., Bonaldo, D., Cassardo, C., Falcieri, F. M., Modugno, G., Russo, A., Sclavo, M., and Carniel, S.: Sensitivity of a Mediterranean Tropical-Like Cyclone to Different Model Configurations and Coupling Strategies, Atmosphere, 8, 92, https://doi.org/10.3390/atmos8050092, 2017.
- Ricchi, A., Miglietta, M. M., Bonaldo, D., Cioni, G., Rizza, U., and Carniel, S.: Multi-Physics Ensemble versus Atmosphere—Ocean Coupled Model Simulations for a Tropical-Like Cyclone in the Mediterranean Sea, Atmosphere, 10, 202, https://doi.org/10.3390/atmos10040202, 2019.
- Ricchi, A., Bonaldo, D., Miglietta, M. M., and Carniel, S.: On the Ocean Mixed Layer influence on the gene-

- sis of Mediterranean Tropical-Like cyclones, EGU General Assembly 2020, Online, 4–8 May 2020, EGU2020-22001, https://doi.org/10.5194/egusphere-egu2020-22001, 2020.
- Rixen, M., Beckers, J.-M., Levitus, S., Antonov, J., Boyer, T., Maillard, C., Fichaut, M., Balopoulos, E., Iona, S., Dooley, H., Garcia, M.-J., Manca, B., Giorgetti, A., Manzella, G., Mikhailov, N., Pinardi, N., and Zavatarelli, M.: The Western Mediterranean Deep Water: A proxy for climate change, Geophys. Res. Lett., 32, https://doi.org/10.1029/2005GL022702, 2005.
- Sanford, T. B., Black, P. G., Haustein, J. R., Feeney, J. W., Forristall, G. Z., and Price, J. F.: Ocean Response to a Hurricane. Part I: Observations, J. Phys. Oceanogr., 17, 2065–2083, https://doi.org/10.1175/1520-0485(1987)017<2065:ORTAHP>2.0.CO;2, 1987.
- Saraceni, M., Silvestri, L., Bechtold, P., and Bongioannini Cerlini, P.: Mediterranean tropical-like cyclone forecasts and analysis using the ECMWF ensemble forecasting system with physical parameterization perturbations, Atmos. Chem. Phys., 23, 13883–13909, https://doi.org/10.5194/acp-23-13883-2023, 2023.
- Scardino, G., Miglietta, M. M., Kushabaha, A., Casella, E., Rovere, A., Besio, G., Borzì, A. M., Cannata, A., Mazza, G., Sabato, G., and Scicchitano, G.: Fingerprinting Mediterranean hurricanes using pre-event thermal drops in seawater temperature, Sci. Rep., 14, 8014, https://doi.org/10.1038/s41598-024-58335-w, 2024.
- Scardino, G., Kushabaha, A., Miglietta, M. M., Bonaldo, D., and Scicchitano, G.: When Storms Stir the Mediterranean Depths: Chlorophyll-a Response to Mediterranean Cyclones, Zenodo [data set], https://doi.org/10.5281/zenodo.15912789, 2025.
- Scicchitano, G., Scardino, G., Monaco, C., Piscitelli, A., Milella, M., De Giosa, F., and Mastronuzzi, G.: Comparing impact effects of common storms and Medicanes along the coast of south-eastern Sicily, Mar. Geol., 439, 106556, https://doi.org/10.1016/j.margeo.2021.106556, 2021.
- Shay, L. K., Black, P. G., Mariano, A. J., Hawkins, J. D., and Elsberry, R. L.: Upper ocean response to Hurricane Gilbert, J. Geophys. Res.-Oceans, 97, 20227–20248, https://doi.org/10.1029/92JC01586, 1992.
- Skliris, N., Sofianos, S., Gkanasos, A., Mantziafou, A., Vervatis, V., Axaopoulos, P., and Lascaratos, A.: Decadal scale variability of sea surface temperature in the Mediterranean Sea in relation to atmospheric variability, Ocean Dynam., 62, 13–30, https://doi.org/10.1007/s10236-011-0493-5, 2012.
- Suzuki, S., Niino, H., and Kimura, R.: The mechanism of upper-oceanic vertical motions forced by a moving typhoon, Fluid Dynam. Res., 43, 025504, https://doi.org/10.1088/0169-5983/43/2/025504, 2011.
- Tartaglione, N., Speranza, A., Dalan, F., Nanni, T., Brunetti, M., and Maugeri, M.: The mobility of Atlantic baric depressions leading to intense precipitation over Italy: a preliminary statistical analysis, Nat. Hazards Earth Syst. Sci., 6, 451–458, https://doi.org/10.5194/nhess-6-451-2006, 2006.

- Teruzzi, A., Bolzon, G., Feudale, L., and Cossarini, G.: Deep chlorophyll maximum and nutricline in the Mediterranean Sea: emerging properties from a multi-platform assimilated biogeochemical model experiment, Biogeosciences, 18, 6147–6166, https://doi.org/10.5194/bg-18-6147-2021, 2021.
- Tiesi, A., Pucillo, A., Bonaldo, D., Ricchi, A., Carniel, S., and Miglietta, M. M.: Initialization of WRF Model Simulations With Sentinel-1 Wind Speed for Severe Weather Events, Front. Mar. Sci., 8, https://doi.org/10.3389/fmars.2021.573489, 2021.
- Vargas-Yáñez, M., Moya, F., Balbín, R., Santiago, R., Ballesteros, E., Sánchez-Leal, R. F., Romero, P., and García-Martínez, M. C.: Seasonal and Long-Term Variability of the Mixed Layer Depth and its Influence on Ocean Productivity in the Spanish Gulf of Cádiz and Mediterranean Sea, Front. Mar. Sci., 9, 901893, https://doi.org/10.3389/fmars.2022.901893, 2022.
- Varlas, G., Vervatis, V., Spyrou, C., Papadopoulou, E., Papadopoulos, A., and Katsafados, P.: Investigating the impact of atmosphere–wave–ocean interactions on a Mediterranean tropical-like cyclone, Ocean Modell., 153, 101675, https://doi.org/10.1016/j.ocemod.2020.101675, 2020.
- Walker, N. D., Leben, R. R., and Balasubramanian, S.: Hurricane-forced upwelling and chlorophyll *a* enhancement within cold-core cyclones in the Gulf of Mexico, Geophys. Res. Lett., 32, https://doi.org/10.1029/2005GL023716, 2005.
- Wang, Y.: Composite of Typhoon-Induced Sea Surface Temperature and Chlorophyll-*a* Responses in the South China Sea, J. Geophys. Res.-Oceans, 125, e2020JC016243, https://doi.org/10.1029/2020JC016243, 2020.
- Wu, Y., Platt, T., Tang, C., and Sathyendranath, S.: Short-term changes in chlorophyll distribution in response to a moving storm: A modelling study, Mar. Ecol.-Prog. Ser., 335, 57–68, https://doi.org/10.3354/meps335057, 2007.
- Yang, C.-Y., Yang, Y. J., Tseng, Y.-H., Jan, S., Chang, M.-H., Wei, C.-L., and Terng, C.-T.: Observational evidence of overlooked downwelling induced by tropical cyclones in the open ocean, Sci. Rep., 14, 335, https://doi.org/10.1038/s41598-023-51016-0, 2024.
- Zhang, H., He, H., Zhang, W.-Z., and Tian, D.: Upper ocean response to tropical cyclones: a review, Geosci. Lett., 8, 1, https://doi.org/10.1186/s40562-020-00170-8, 2021.
- Zhao, H., Tang, D., and Wang, Y.: Comparison of phytoplankton blooms triggered by two typhoons with different intensities and translation speeds in the South China Sea, Mar. Ecol.-Prog. Ser., 365, 57–65, https://doi.org/10.3354/meps07488, 2008.